

WIRELESS ENGINEER

Vol. XXVI

NOVEMBER 1949

No. 314

Axial Field of a Helix

WHEN establishing the formula for the magnetic field on the axis of a solenoid, one can either write down the expression for the field at any point on the axis of a single turn and integrate it over the length of the coil, or what is simpler, assume a unit pole to be moved, say, a distance of 1 cm along the axis. In the latter case, if the coil is infinitely long, every one of the 4π lines will cut as many turns as there are in a centimetre, and the work done will be

$H = 4\pi \times \frac{I}{10} \times \text{turns per cm.}$ We are speaking in terms of the classical c.g.s. system. If the pole is placed exactly at one end of the coil, the other end of which is far away, exactly 2π of the 4π lines will cut the turns and H will be half this value. If the coil is relatively short exactly the same method can be employed if we determine what fraction of the 4π lines cuts the turns when the pole is given a small axial movement. To determine H at the centre, the simplest method of

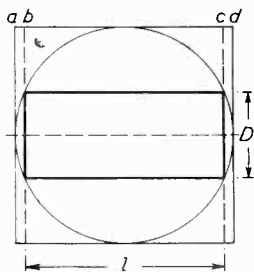
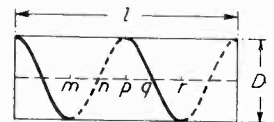


Fig. 1

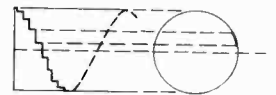
doing this is shown in Fig. 1, where a sphere is drawn with its surface passing through the ends of the coil. The fraction of the total flux emanating from the pole which cuts the winding and does not escape at the ends is the same as the fraction of the total spherical surface which lies outside the cylindrical surface of the coil. Since the areas of the spherical surfaces are equal to the corresponding areas of the cylinder that embraces the

sphere, this fraction is simply bc/ad , where bc is the length l of the coil and ad is the diameter of the sphere, which is equal to $\sqrt{l^2 + D^2}$. Hence H at the centre of the coil is equal to what it would be if the coil were infinitely long multiplied by $l/\sqrt{l^2 + D^2}$.

So far this has been ordinary routine procedure, but difficulties arise if, instead of a closely-wound coil, one considers a very open helix as shown in Fig. 2(a). On placing a unit pole on the axis and moving it a short distance, a student would be justified in pointing out that very few of the 4π lines will cut the turns of the coil, even if it is infinitely long. This objection can be met in several ways; although very few of the lines emanating from the pole will cut the turns, those that do, cut a current correspondingly concentrated, so that the product of flux and current cut by the movement is the same as it would be if the current were uniformly distributed over the surface, so long as the ampere-turns per centimetre remain the same.



(a)



(b)

Fig. 2

Another way of saying the same thing is shown in Fig. 2(b) where the helical winding is replaced by a stepped winding consisting of alternate axial and circumferential sections. The axial sections produce no axial field, and it is only field in the axial direction that we are considering, but each circumferential section produces exactly the same axial field as it would do if it were a

complete turn, with the current correspondingly reduced. Hence, so far as the axial field—that is, both at the axis and in the direction of the axis,—is concerned, the two turns in Fig. 2(a) can be replaced by twenty turns carrying a tenth of the current. This does not apply to any point not on the axis, and even on the axis it only applies to the axial component of the field. With widely-spaced turns as in Fig. 2(a) there will be at the axis a component field normal to the radius to the coil at that point, due to the

axial component of the winding. At m it will be normal to the paper, at n in the plane of the paper, at p normal to the paper but opposite to what it was at m , and so on, proceeding with a screw-like motion along the axis. The resultant field at any point of the axis is the resultant of the axial and radial components, both of which can be determined without much difficulty but as soon as one leaves the axis the difficulties increase enormously.

G. W. O. H.

CONTOUR ANALYSIS OF MIXER VALVES

By N. E. Goddard, B.A.

(Mullard Electronic Research Laboratory)

SUMMARY : The characteristics of a mixer valve are completely defined by a series of three-dimensional surfaces. Two of the co-ordinates, grid voltage and heterodyne-oscillator voltage, determine the operating conditions for small signal voltages. The third co-ordinate is one of a number of valve parameters; fundamental or harmonic conversion conductance, cathode current or grid current. Each surface is described by a contour map on which load lines are drawn for several automatic-bias circuits. The method is illustrated by Fourier analysis of a theoretical mutual-conductance curve and by experimental measurements on an EF42 pentode.

1. Introduction

THE problems associated with the operation of frequency changers and mixers for superheterodyne receivers have been described by various authors, notably Herold.¹ The analysis of a frequency changer is more complex than that of an amplifier because its operation is essentially non-linear and because the signal and heterodyne voltages produce modulation products and interaction between their respective circuits. The overall performance must, therefore, be assessed in terms of various factors which include conversion conductance, input and output impedances, noise, harmonic interference, inter-electrode impedances, transit-time effects and oscillator stability. This paper is mainly concerned with the conversion conductance, which is the basic characteristic.

The conversion conductance of a mixer may be determined in two ways; theoretically, by mathematical analysis of the static characteristics and practically, by direct measurement. A survey of numerous mathematical methods² leads to the conclusion that a computation office is required to handle the mass of calculations that result from a general approach to the problem. The practical method is, therefore, more convenient.

Unfortunately, the practical curves usually available give only a limited amount of information, and performance figures for the same valve, but for different circuits, are not related.

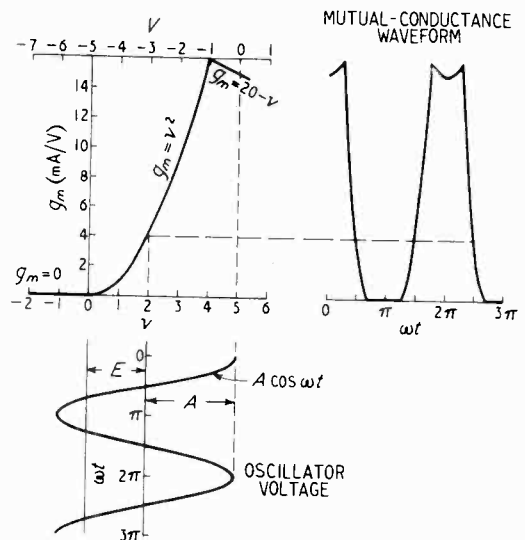


Fig. 1. Mutual-conductance curves; grid voltage v is referred arbitrarily to the cut-off point. The total voltage applied is $A \cos \omega t + E$.

MS accepted by the Editor. February 1949

The conventional method of presenting mixer characteristics is a graph showing conversion conductance plotted against oscillator voltage. This method is adequate in published data in which the details of a preferred circuit

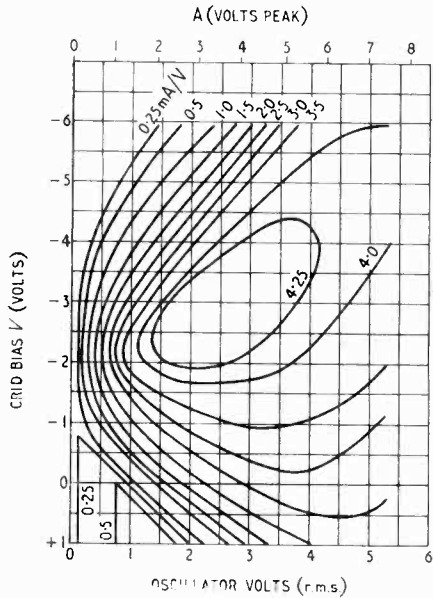


Fig. 2. Theoretical conversion-conductance contours. The contours are calculated from the mutual-conductance waveform in Fig. 1, but the grid bias V is referred to $v = 5$ of Fig. 1 as origin.

are given, but it does not allow the calculation of performance figures for a non-standard circuit and does not give a graphical picture of the changes involved in variations of circuit values. The contour method has been devised in order to avoid these disadvantages and to facilitate a precise comparison of diverse automatic-bias circuits.

The method is illustrated by Fourier analysis of a hypothetical mutual-conductance curve and by experimental measurements on an EF42 pentode. The performance figures for a variety of circuits can be calculated from the practical curves and the conversion conductance for first, second and third harmonic operation deduced.

2. Conversion - Conductance Contours — Theoretical Analysis

The general analysis of a mixer is independent of the relative positions of the signal and oscillator grids. Thus the operation of an additive mixer, in which both voltages are applied to the same grid, is treated in the same way as a multiplicative mixer, in which the voltages are applied

to different grids. The circuit is considered as an amplifier in which the signal-grid mutual conductance varies with time in a manner determined by the heterodyne-oscillator voltage only. In other words, it is assumed that the signal voltage is very small compared with the oscillator voltage. The conversion conductance is then calculated from the component of output current at the intermediate frequency.

The signal-grid mutual conductance may be written as a Fourier series, since its variation with time is periodic¹

$$g_m = a_0 + a_1 \cos \omega t + a_2 \cos 2 \omega t + \dots \quad (1)$$

where ω is the angular frequency of the oscillator voltage and a_0, a_1, a_2 are the Fourier coefficients. If the signal voltage is $e \sin pt$, then the output current, usually the anode current, is given by

$$\begin{aligned} i &= g_m e \sin pt \\ &= a_0 e \sin pt + e \sum_{n=1}^{\infty} a_n \sin pt \cos n\omega t \\ &= a_0 e \sin pt + \frac{1}{2} e \sum_{n=1}^{\infty} a_n \sin (p + n\omega) t \\ &\quad + \frac{1}{2} e \sum_{n=1}^{\infty} a_n \sin (p - n\omega) t \\ &\quad \dots \dots \dots \quad (2) \end{aligned}$$

The component of anode current containing terms of angular frequency $(p \sim n\omega)^*$ is the intermediate-frequency output current (i_{if}). If the intermediate frequency is ω_i , then

$$p = n\omega \pm \omega_i$$

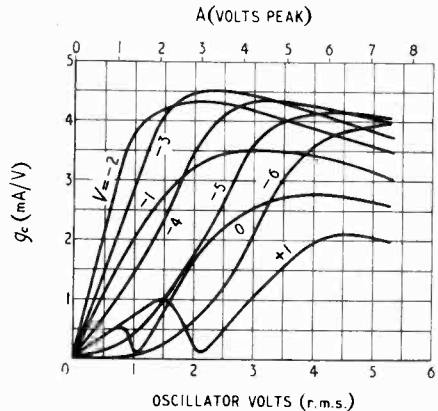


Fig. 3. Theoretical conversion-conductance profiles. Maximum value of g_c for an ideal step characteristic with $g_o = 16 \text{ mA/V}$ is g_o/π or 5.1 mA/V .

and since n is an integer, the same intermediate frequency will be produced by pairs of signal frequencies, spaced ω_i on either side of each harmonic of the oscillator frequency. The harmonics are generated in the mixer itself and

* The symbol \sim is used to denote 'the difference between the quantities designated without regard to sign'.

need not exist in the oscillator voltage. The conversion conductance at the n th harmonic is

$$g_{cn} = \frac{i_{if}}{e} = \frac{a_n}{2} \dots \dots \dots (3)$$

i.e., the conversion conductance is equal to half the n th coefficient in the Fourier series for the waveform representing the variation of mutual conductance with time (Fig. 1) thus

$$g_{cn} = \frac{I}{2\pi} \int_0^{2\pi} g_m \cos n\omega t d(\omega t) \dots \dots (4)$$

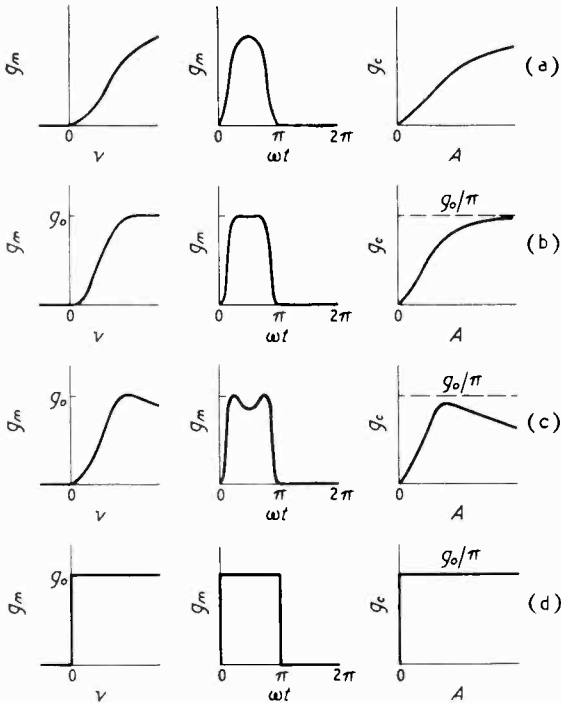


Fig. 4. Mutual-conductance waveforms and conversion-conductance curves for four hypothetical mutual-conductance characteristics (bias fixed at cut-off).

Since the instantaneous value of the mutual conductance, g_m , is a function of the voltage, v , on the grid to which the oscillator voltage is applied, therefore

$$g_{cn} = \frac{I}{2\pi} \int_0^{2\pi} f(v) \cos n\omega t d(\omega t) \dots \dots (5)$$

The grid voltage, v , is itself a function of the steady bias and the oscillator voltage which, therefore, uniquely determine the conversion conductance for a given set of circuit conditions. It is assumed that the operating voltages on the remaining electrodes remain constant.

It follows that the important characteristic of a mixer valve is a three-dimensional surface in a conversion conductance, grid voltage and oscil-

lator voltage co-ordinate system. The surface may be imagined with the grid voltage and oscillator voltage axes in a horizontal plane and the conversion conductance axis vertical. The mixer characteristic usually quoted for a preferred circuit is the projection, on a conversion-conductance/oscillator-voltage plane, of a line on the surface whose projection on a horizontal plane is a curve representing the variation of grid voltage with oscillator voltage for that particular circuit.

Conversion-conductance contours are curves of intersection with horizontal planes and, therefore, form a contour map of the characteristic surface. The operating condition in a particular application is determined by finding a point on the map at which the conversion conductance and its rate of change with bias and oscillator voltage have the desired values. A more detailed discussion of this question is given in Section 3.

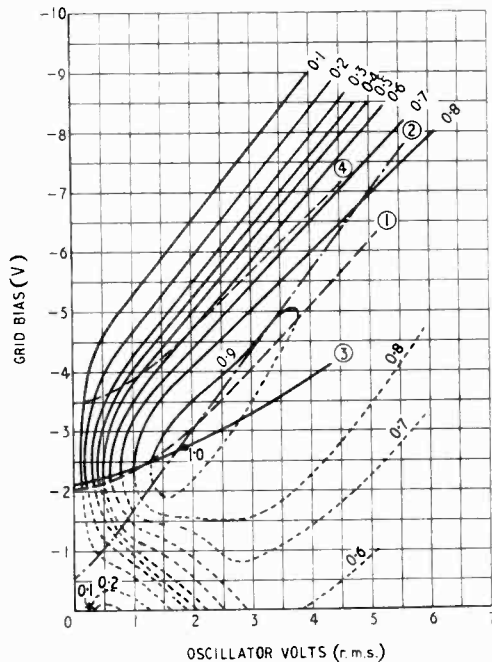


Fig. 5. Fundamental conversion-conductance contours: (1) 10-mA anode current curve, (2) 1-MΩ grid leak, (3) 200-Ω cathode resistor, (4) 1,350-Ω cathode resistor. ----- excessive cathode current; (EF42; $V_a = V_{g2} = 250$ V).

The advantages of this method of presentation are twofold. First, it is possible to obtain a clearer picture of a three-dimensional surface from a contour map (Fig. 2) than from a series of profiles such as those of Fig. 3. The second advantage arises from the use of automatic-bias circuits and is discussed in Section 3.

To obtain an idea of the general shape of the conversion-conductance contours, consider the mutual-conductance curve shown in Fig. 1. This composite curve contains three discontinuous sections represented by the equations:—

$$g_m = 0 \quad \text{for } -\infty \leq v \leq 0 \dots \dots (6)$$

$$g_m = v^2 \quad \text{for } 0 \leq v \leq 4 \dots \dots (7)$$

$$g_m = 20 - v \quad \text{for } 4 \leq v \leq 20 \dots \dots (8)$$

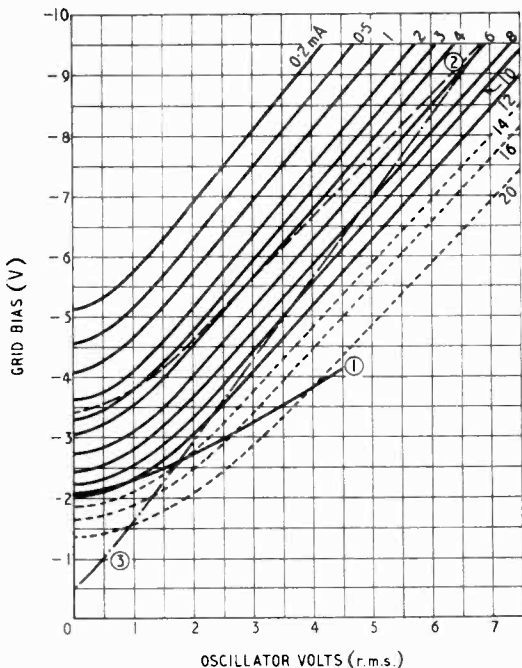


Fig. 6. Cathode-current contours; (1) 200-Ω cathode resistor, (2) 1,350-Ω cathode resistor, (3) 1-MΩ grid leak. ----- excessive cathode current.

grid bias V of -1 V and approximately coincides with the start of grid current in a typical valve.

The contours of Fig. 2 are very useful for comparison with experimental curves. The more important features are as follows:—

- (a) The maximum value of g_c occurs in the region $A = 3$ V, $V = -2.75$ V.

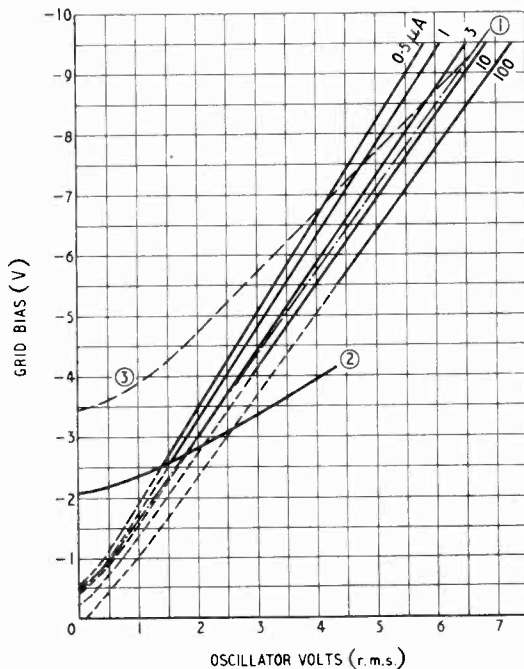


Fig. 7. Grid-current contours; (1) 1-MΩ grid leak, (2) 200-Ω cathode resistor, (3) 1,350-Ω cathode resistor. ----- excessive cathode current.

The variation of mutual conductance with time is obtained by projecting the oscillator-voltage waveform on the mutual-conductance characteristic.

For convenience in calculation, the grid voltage v is referred to the mutual-conductance cut-off point as origin. The heterodyne-oscillator voltage is $A \cos \omega t$ and the steady grid voltage is E . The total voltage at the control grid is therefore $v = A \cos \omega t + E$, and conversion-conductance contours for the hypothetical mutual-conductance curve may be calculated by substitution in equation (5). The necessary formulae are given in the appendix.

The profile curves are plotted in Fig. 3 and the contours in Fig. 2. The grid-bias voltage V is referred to $v = 5$ as origin in order to simulate more closely a practical valve characteristic. The discontinuity at $v = 4$ then occurs at a

- (b) With large negative bias and oscillator voltages g_c changes slowly.
- (c) Changes in g_c are most rapid for small oscillator voltages and $V = 2$ V.
- (d) In the zero-bias region there is a steep trough corresponding to an oscillator voltage swing about the discontinuity at $v = 4$.

Features (a) and (d) are associated with a mutual-conductance characteristic in which g_m reaches a maximum value and decreases in the positive grid-voltage region. It can easily be shown that if the anode-current/grid-voltage characteristic of the valve is a continuous function and the cathode can be saturated, then there must be a point of inflexion at which the mutual conductance is a maximum. In pentodes the decrease in g_m at positive grid voltages may be accentuated by secondary emission. The fact that a conversion-

conductance characteristic with a maximum value is always associated with a similar mutual-conductance characteristic is illustrated in Fig. 4. Four hypothetical mutual-conductance curves are shown, with the corresponding mutual-conductance waveforms and conversion-conductance characteristics for fixed bias-voltage. Fig. 4(c) corresponds to a practical case and 4(d) is an ideal characteristic. In 4(b) a very large oscillator voltage produces a square waveform and a conversion conductance which is asymptotic to a value g_0/π where g_0 is the maximum value of g_m . In 4(c) a very large oscillator voltage drives the valve into anode-current saturation, the mutual-conductance waveform degenerates into a series of progressively narrowing pulses and the conversion conductance tends to zero. The ideal mixer valve would have the characteristics shown in 4(d), in which the mutual-conductance curve is a step. In this case the mutual-conductance

are fixed, the maximum first harmonic or fundamental occurs when the waveform is square.

It follows from this argument that the contours for a practical valve are closed curves.

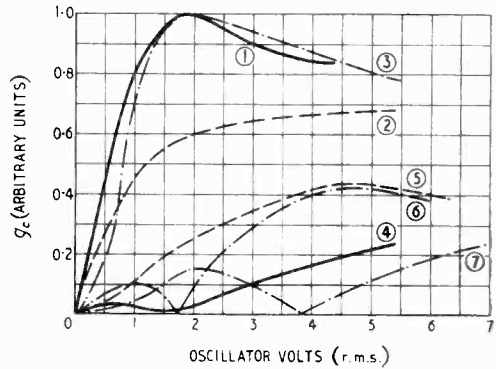


Fig. 9. Conversion-conductance characteristics; (1) fundamental, 200- Ω cathode resistor, (2) fundamental, 1,350- Ω cathode resistor, (3) fundamental, 1-M Ω grid leak, (4) 2nd harmonic, 200- Ω cathode resistor, (5) 2nd harmonic, 1,350- Ω cathode resistor, (6) 2nd harmonic, 1-M Ω grid leak, (7) 3rd harmonic, 1-M Ω grid leak. Curves for a combination of a 200- Ω cathode resistor and 1-M Ω grid-leak resistor follow the full lines up to the start of the grid current (1.25 V r.m.s.) and then approach the grid leak curves.

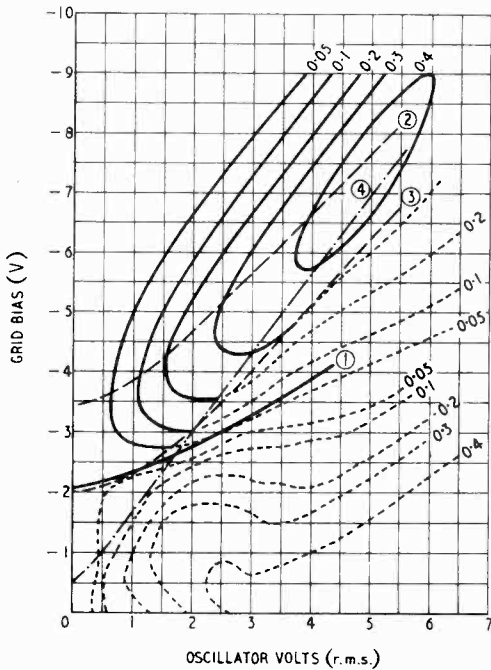


Fig. 8. Second-harmonic conversion-conductance contours: (1) 200- Ω cathode resistor, (2) 1,350- Ω cathode resistor, (3) 10-mA anode current curve, (4) 1-M Ω grid leak. ----- excessive cathode current.

waveform is square for all values of oscillator voltage which are large compared with the signal voltage. The conversion conductance with a characteristic of this shape is the maximum that can be obtained with a given value of g_0 , for when the peak value and period of a waveform

3. Conversion-Conductance Contours

Some experimental contours are shown in Fig. 5. The mixer valve was a television pentode, EF42, with common-grid injection of the signal and oscillator voltages. Signal and oscillator frequencies were 45 Mc/s and 32 Mc/s.

The similarity between the measured contours and the theoretical contours is self-evident, though no attempt was made to align the theoretical mutual-conductance characteristic with that of the EF42. The peak conversion conductance, denoted by contour 1.0 is nearly 4 mA/V. The region in which the rated anode current of 10 mA is exceeded is marked with broken contour lines.

In a majority of mixer circuits the working-bias voltage is derived from an electrode current which is in turn a function of the oscillator voltage. This method is used in preference to fixed bias since it renders the circuit less susceptible to voltage variations and is usually more economical. Typical examples are the use of a grid-leak resistor or cathode resistor or a combination of both in a circuit in which the signal and oscillator voltages are applied simultaneously to the control grid. A curve representing grid voltage as a function of oscillator voltage determines the possible operating conditions of the mixer for a particular bias circuit. Since this

curve has the same coordinates as the contours it may be conveniently superimposed on them as a 'load line' (Fig. 5). The conversion conductance obtained with a given oscillator voltage may be read off directly, and a conventional conversion-conductance characteristic drawn (Fig. 9). The load lines for different values of grid leak and cathode resistor illustrate the different characteristics obtained with these circuits.

Two additional sets of contours are required for calculating the optimum bias resistances. Fig. 6 is a set of cathode-current contours plotted on the same co-ordinates as the conversion-conductance contours. The co-ordinates of the conversion-conductance peak value are (1.8, -2.7). Referring to Fig. 6 the cathode current at this point is 13.5 mA. The cathode resistor to produce 2.7 V bias is therefore 200 Ω . By assuming further values of cathode current and calculating the voltage across 200 Ω , the load line (1) of Fig. 6 is drawn. This is then transferred to Fig. 5 and the conversion conductance characteristic, curve 1 of Fig. 9, is obtained. The corresponding cathode-current curve (Fig. 10) is drawn from Fig. 6.

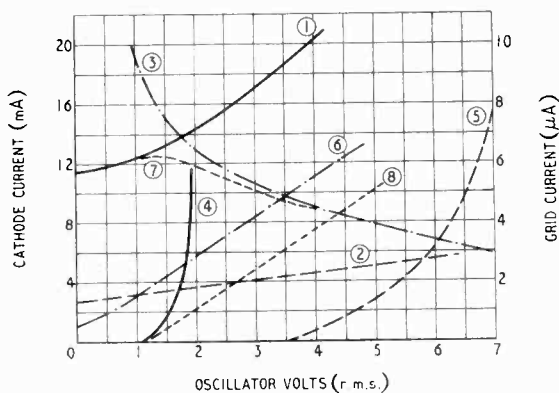


Fig. 10. Cathode and grid-current characteristics; (1) cathode current, 200- Ω cathode resistor, (2) cathode current, 1,350- Ω cathode resistor, (3) cathode current, 1-M Ω grid leak, (4) grid current, 200- Ω cathode resistor, (5) grid current, 1,350- Ω cathode resistor, (6) grid current, 1-M Ω grid leak, (7) cathode current, 200- Ω cathode resistor and 1-M Ω grid leak, (8) grid current, 200- Ω cathode resistor and 1-M Ω grid leak.

With grid-leak bias, the optimum resistance is derived in a similar way from the grid-current contours in Fig. 7. The optimum value is approximately 1 M Ω and, by transferring the calculated load line to Figs. 5 and 6, the conversion-conductance and cathode-current curves in Fig. 9 and 10 are drawn. The grid-current curves for both cathode-resistor and grid-leak bias are obtained from Fig. 7. Thus, by using

three sets of contour curves, the complete characteristics for any value of cathode or grid resistor can be calculated.

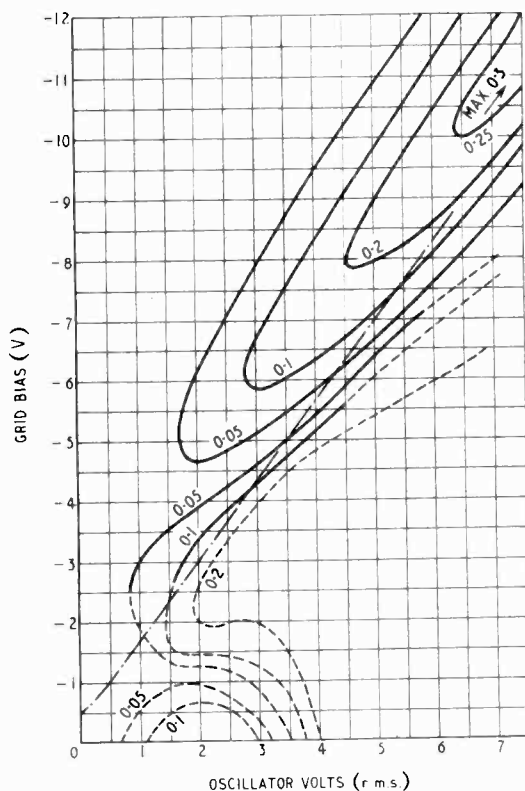


Fig. 11. Third-harmonic conversion-conductance contours; ——— 1-M Ω grid leak, - - - excessive cathode current.

Fig. 10 shows that the change in cathode current with increasing oscillator voltage is positive with a cathode resistor and negative with a grid resistor. The corresponding load lines in Fig. 6 cross the cathode-current contours in opposite directions. In both cases the cathode current exceeds the rated value over part of the load line. It can be maintained within the rated value for all values of oscillator voltage by using both cathode and grid resistors simultaneously. Referring to Fig. 10, the cathode current follows curve 1 from zero oscillator voltage up to the point where grid current starts to flow; it then becomes asymptotic to curve 3. The conversion-conductance characteristic is a similar combination of curves 1 and 3 in Fig. 9.

So far only the fundamental conversion conductance has been discussed. The contour analysis is equally applicable to harmonic conversion and Fig. 8 is a set of experimental contours for 2nd-harmonic mixing using a signal frequency

of 77 Mc/s ($2\omega + \omega_i$), heterodyne frequency 32 Mc/s, and intermediate frequency 13 Mc/s. It is immediately apparent that much higher oscillator and bias voltages are required for optimum performance. A further point of interest is the steep trough which passes through the point for maximum fundamental conversion conductance. The peak conversion conductance for second-harmonic operation is nearly 2 mA/V.

The optimum bias resistors are calculated by the method used for fundamental operation. A 1-M Ω grid resistor gives a load line (curve 4, Fig. 8) which passes close to the peak value. Curve 2 of Fig. 8 is a load line for a 1,350- Ω cathode resistor. The 200- Ω cathode-resistor load line is also drawn on these contours to give the possible second-harmonic interference level when fundamental mixing is used.

Contours for third-harmonic mixing (signal frequency $3\omega \pm \omega_i$) are given in Fig. 11. The main peak is fairly flat at 0.3 of the peak fundamental conversion conductance and in the region of coordinates (10, -14.5). The main trough, which is very steep, passes through the optimum working point for second-harmonic mixing. The relative peak-conversion conductance values for the three harmonics (1.0, 0.45, 0.3) illustrate the approximate rule that the peak value is inversely proportional to the order of the harmonic.

4. Conclusions

The complete conversion characteristics of a mixer valve are most conveniently presented in the form of contour maps. A set of contours can be drawn up for each electrode current and a load line calculated for any given bias circuit through which the current passes. This load line is then transposed on to the remaining sets of contours and the appropriate characteristics for the electrode currents and for the conversion conductance at any harmonic frequency can be derived. The optimum bias circuits can be accurately calculated and the effect of circuit variations rapidly deduced.

5. Acknowledgments

The work described in this paper was carried out at the Mullard Electronic Research Laboratory and permission to publish is gratefully acknowledged. The author is indebted to Dr. C. F. Bareford and Mr. M. G. Kelliher for valuable criticism and encouragement.

APPENDIX

The Fourier analysis of the mutual-conductance waveform is divided into five parts as the oscillator voltage drives the grid over one, two or three of the ranges represented by the component functions:

(a) $g_m = 0$; $g_m = v^2$.

Integration over $g_m = 0$ gives no contribution to the conversion conductance. The limits are, therefore, defined by $\omega t = 0$, $A \cos \omega t + E = 0$, where E is the working grid voltage relative to the origin. If $\alpha = \cos^{-1}(-E/A)$,

$$\pi g_c = \int_0^\alpha (A \cos \omega t + E)^2 \cos \omega t d(\omega t) \dots \dots (9)$$

$$= \frac{(E^2 + 2A^2) \sqrt{A^2 - E^2}}{3A} + AE \cos^{-1}(-E/A) \quad (10)$$

(b) $g_m = v^2$

The limits of integration are 0 and 2π

$$\pi g_c = \frac{1}{2} \int_0^{2\pi} (A \cos \omega t + E)^2 \cos \omega t d(\omega t) \dots \dots (11)$$

$$g_c = AE \dots \dots \dots (12)$$

(c) $g_m = v^2$; $g_m = 20 - v$.

The limits for $g_m = v^2$ are $A \cos \omega t + E = 4$, $\omega t = \pi$ and for $g_m = 20 - v$; $\omega t = 0$, $A \cos \omega t + E = 4$.

Let $\beta = \cos^{-1} \frac{4-E}{A}$

$$\pi g_c = \int_0^\beta [20 - (A \cos \omega t + E)] \cos \omega t d(\omega t)$$

$$+ \int_\beta^\pi (A \cos \omega t + E)^2 \cos \omega t d(\omega t) \dots \dots (13)$$

$$= AE\pi - A(E + \frac{1}{2}) \cos^{-1} \left(\frac{4-E}{A} \right)$$

$$- \frac{\sqrt{A^2 - (4-E)^2}}{3A} (2A^2 + E^2 + 11E/2 - 38) \quad (14)$$

(d) $g_m = 0$; $g_m = v^2$; $g_m = 20 - v$

The limits are $0 - \beta$ and $\beta - \alpha$ with the same integrals as (13)

$$\pi g_c = \frac{1}{3A} \left[(E^2 + 2A^2) \sqrt{A^2 - E^2} \right.$$

$$\left. - \sqrt{A^2 - (4-E)^2} (2A^2 + E^2 + 11E/2 - 38) \right]$$

$$+ A \left[E \cos^{-1}(-E/A) - (E + \frac{1}{2}) \cos^{-1} \frac{4-E}{A} \right] \quad (15)$$

(e) $g_m = 20 - v$

$$\pi g_c = \frac{1}{2} \int_0^{2\pi} (20 - A \cos \omega t - E) \cos \omega t d(\omega t) \dots (16)$$

$$g_c = A/2$$

Equations 10, 12, 14, 15 and 17 are the equations for the conversion-conductance contours, and by substituting values of E and A Fig. 2 and 3 can be drawn. The grid bias V used in these figures is equal to $E - 5$ (Fig. 1).

REFERENCES

¹ Herold, E. W., *Proc. Inst. Radio Engrs*, Feb. 1942, Vol. 30, p. 84
² Stockman, H., *J. Appl. Phys.*, Feb. 1946, Vol. 17, p. 110.

STAGGER-TUNED LOW-PASS AMPLIFIERS

By W. E. Thomson, M.A.

(P.O. Research Station)

SUMMARY.—The method of design of band-pass amplifiers by stagger-tuning, in its wider sense, may be simply extended to low-pass amplifiers as far as specifying the frequency response is concerned. The determination of networks having this frequency response presents a fresh problem. Suitable networks are given here which allow a multistage low-pass amplifier to be built with a gain, as a voltage ratio, of $g_m/\omega_0 C$ per stage, a bandwidth of $\omega_0/2\pi$ c/s, or slightly more, and a reasonably flat pass-band; g_m is the mutual conductance of the valves used and C the interstage capacitance.

1. Introduction

A METHOD of designing band-pass amplifiers which has received some attention in recent years is that which began with the conception of 'stagger-tuning.' The name has been applied¹ to extensions of the method, even although the circuits involved have not consisted of simple tuned circuits. The essence of the method is that of designing a multistage amplifier as a whole, with stages with different characteristics, these combining to give an overall characteristic better than could be obtained with identical stages.

The problems involved fall into two distinct sections. The first is that of finding a suitable frequency response, which will give the required flatness of gain in a prescribed band; the second is that of determining networks to realize this frequency response. The frequency functions which have been found are also suitable for low-pass amplifiers; all that is required is to set the mid-band frequency equal to zero. The band-pass amplifier circuits cannot be so modified and thus a fresh problem is presented, that of finding networks to realize the low-pass frequency function. A solution to the problem is presented in this paper.

2. Amplifier Gain v. Frequency

This section summarizes briefly the work of previous writers.^{2, 3}

A frequency function in the low-pass form suitable for representing the complex gain of an amplifier (i.e., the complex ratio of output voltage to input voltage) is

$$G = \frac{G_0}{a_n \lambda^n + a_{n-1} \lambda^{n-1} + a_{n-2} \lambda^{n-2} + \dots + a_1 \lambda + a_0} \quad (1)$$

In this expression $\lambda = j\omega$, ω being angular frequency; G_0 is a constant which largely determines

the absolute gain of the amplifier; it is not specified arbitrarily but depends on the mutual conductance of the valves, the interstage shunt capacitance, and the bandwidth. The variation with frequency is controlled by the parameters a_0 to a_n , which are real and positive; n is, in practice, the number of stages in the amplifier. The polynomial which forms the denominator in (1) may be factorized, giving

$$G = \frac{G_0}{a_n (\lambda - b_1) (\lambda - b_2) \dots (\lambda - b_n)} \quad (2)$$

where the constants b_1 to b_n are known as the 'poles' of the gain function. Since the a -terms are real, the b -terms either are real or occur in complex conjugate pairs; for the amplifier to be stable, the real parts of the b -terms must be negative. These poles may also be represented by points on a complex plane, and this representation is very convenient since these points, in the schemes which have been devised, lie on simple geometric curves.

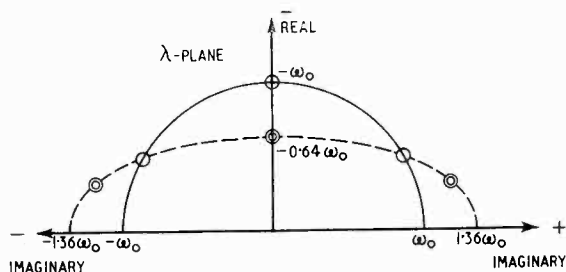


Fig. 1. Location of poles in typical schemes; O poles according to Landon's scheme $n = 3$; ● poles according to Linnebach's scheme $n = 3$, $d = 0.6$.

In Linnebach's scheme² the parameters used are the nominal bandwidth ω_0 , the ripple d , and n . The actual bandwidth is then $2d\omega_0$ and the gain in this pass-band varies over a range of $20 \log_{10} \{(1 + d^{2n})/(1 - d^{2n})\}$ decibels. The poles are then given by

MS accepted by the Editor, March 1949

$$b_m = -[(1 - d^2) \sin \{(2m - 1) \cdot 90^\circ/n\}] \omega_0 + j[(1 + d^2) \cos \{(2m - 1) \cdot 90^\circ/n\}] \omega_0$$

for $m = 1, 2, 3, \dots, n$.

The corresponding points on the complex plane lie on the ellipse with semi-major axis $(1 + d^2)\omega_0$ coinciding with the imaginary axis and semi-minor axis $(1 - d^2)\omega_0$ coinciding with the real axis. Fig. 1 shows the location of these poles for $n = 3$ and $d = 0.6$; so that

$$b_1 = -0.32\omega_0 + j0.68\sqrt{3}\omega_0; \quad b_2 = -0.64\omega_0; \\ b_3 = -0.32\omega_0 - j0.68\sqrt{3}\omega_0.$$

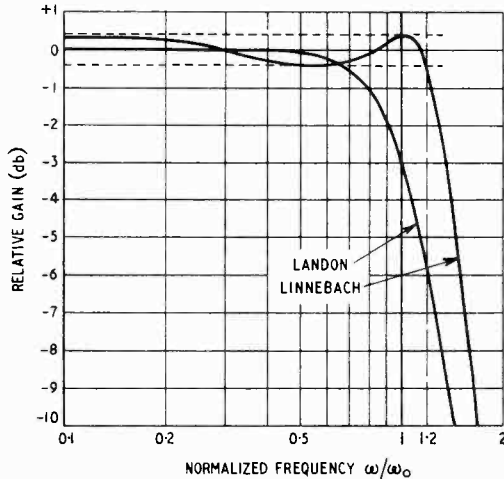


Fig. 2. Gain-frequency responses associated with pole distributions of Fig. 1.

The corresponding gain is found by substituting these values in (2), with $a_n = a_3 = 1/\omega_0^3$, replacing λ by $j\omega$ and finding the modulus in the usual way; the result is

$$\text{Gain} = 20 \log_{10} G_0 - 10 \log_{10} \left\{ (1 - d^6)^2 + 9d^4(\omega/\omega_0)^2 - 6d^2(\omega/\omega_0)^4 + (\omega/\omega_0)^6 \right\} \text{ decibels} \quad (4)$$

The second term, with $d = 0.6$, is shown in Fig. 2. It varies, up to $1.2\omega_0$, between $20 \log_{10} (1 - d^6)$ and $20 \log_{10} (1 + d^6)$; i.e., between about ± 0.4 decibel.

Landon's scheme³ may be regarded as the limiting case of Linnebach's when $d = 0$; although this gives the apparently useless result of zero variation of gain with zero bandwidth the scheme is nevertheless useful. The result of putting $d = 0$ in equation (4) is

$$\text{Gain} = 20 \log_{10} G_0 - 10 \log_{10} \{1 + (\omega/\omega_0)^6\} \quad (5)$$

The corresponding curve is also shown in Fig. 2. The gain falls gradually without any ripple and is 3 db down at the nominal cut-off ω_0 . This is true for all values of n . The poles, at $b = -\omega_0$, $b = (-\frac{1}{2} \pm j\sqrt{3}/2)\omega_0$, are shown in Fig. 1. They lie on the circle with centre at the origin and radius ω_0 .

3. Practical Amplifier Networks

3.1 General.

The representation of the complex gain in equation (2) shows that the total gain may be expressed as a product of factors of two types

$$(a) \frac{b_r G_r}{\lambda - b_r}; \quad (b) \frac{b_s b_s^* G_s}{(\lambda - b_s)(\lambda - b_s^*)}$$

where b_r is a real number and b_s and b_s^* are a conjugate complex pair of numbers. If n is odd there is one factor of type (a) and $(n - 1)/2$ factors of type (b); if n is even there are $n/2$ factors of type (b).

If circuits can be found with complex gain functions of these types and these units can be connected in tandem so that the total complex gain is the product of individual gains the problem is solved. The following sections deal with such units.

3.2 Type (a) gain function.

As pointed out by Landon, the type (a) gain function may be realized in terms of the voltage across a resistor and capacitor in parallel fed from a constant-current source. This is illustrated by an outline circuit in Fig. 3. The constant-current generator is provided by a pentode valve so that the gain is $g_m Z$, where g_m is the mutual conductance of the valve and Z the impedance of the load.

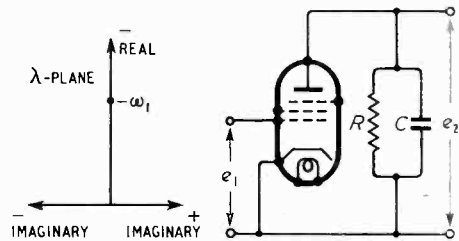


Fig. 3. Realization of gain function with single pole at $\lambda = -\omega_1$.

$$R = \frac{1}{\omega_1 C}, \quad \text{gain} = -\frac{e_2}{e_1} = \frac{g_m}{\omega_1 C} \cdot \frac{\omega_1}{\lambda + \omega_1}$$

3.3 Type (b) gain function.

Landon gives a circuit which involves a single valve with a four-terminal load in order to obtain a type (b) gain function. As he points out, the load has shunt capacitance across one pair of terminals only and is thus not suitable for a wideband amplifier. A solution which avoids this difficulty is shown in Fig. 4. Two valve stages are required, each having two-terminal loads: The first has a resistive load shunted by a capacitor; the second has an inductance-compensated load as commonly used

in wideband amplifiers. The gain of such a pair of stages would in general be

$$\frac{g_m R_1}{1 + \lambda C R_1} \cdot \frac{g_m (R_2 + \lambda L)}{1 + \lambda C R_2 + \lambda^2 L C}$$

The values of g_m and C have been taken as equal in the two stages, for simplicity, but it is not necessary that they should be equal. The com-

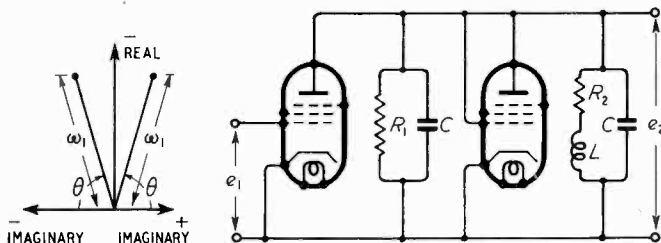


Fig. 4. Realization of gain function with conjugate complex pair of poles at $\lambda =$

$$-\omega_1 \sin \theta \pm j\omega_1 \cos \theta. \quad R_1 = \frac{1}{2 \sin \theta \cdot \omega_1 C},$$

$$R_2 = \frac{2 \sin \theta}{\omega_1 C}, \quad L = \frac{1}{\omega_1^2 C}, \quad \text{gain} = \frac{e_2}{e_1} =$$

$$\left(\frac{g_m}{\omega_1 C}\right)^2 \frac{\omega_1^2}{\lambda^2 + 2\omega_1 \sin \theta \cdot \lambda + \omega_1^2}$$

ponents R_2 and L are chosen so that the factor $1 + \lambda C R_2 + \lambda^2 L C$ gives the wanted values of b_s and b_s^* ; R_1 is then chosen so that the factor $R_2 + \lambda L$ is R_2 times the factor $1 + \lambda C R_1$. The whole expression then reduces to the required form with

$$b_s = -\omega_1 \sin \theta + j\omega_1 \cos \theta;$$

$$b_s^* = -\omega_1 \sin \theta - j\omega_1 \cos \theta.$$

4. Complete Amplifiers

When n and d , and hence the poles, have been specified for a complete amplifier, the amplifier is made up of units, as described in Section 3, connected in tandem. The nominal gain (as a voltage ratio), G_0 in equations (1) and (2) is $(g_m/\omega_0 C)^n$, or if g_m and C differ in different stages is the product of n factors, $g_m/\omega_0 C$, each with its appropriate values of g_m and C . For normal values of n and d , the mean gain in the pass-band (in logarithmic units) will differ inappreciably from $20 \log_{10} G_0$.

Fig. 5 shows outline circuit diagrams and component formulae for two three-stage amplifiers corresponding to the pole distributions of Fig. 1 and the frequency-responses of Fig. 2. The first stage may be regarded as realizing the real pole and the last two as realizing the complex pair of poles. The fact that the first two stages are identical is associated with the fact that $n=3$ and is not true in general. If the capacitance differs, each component is calculated from the capacitance for its own stage.

There are two practical difficulties which amplifiers of this type share with stagger-tuned amplifiers in general. First, the way in which the amplifier overloads depends on the order of the

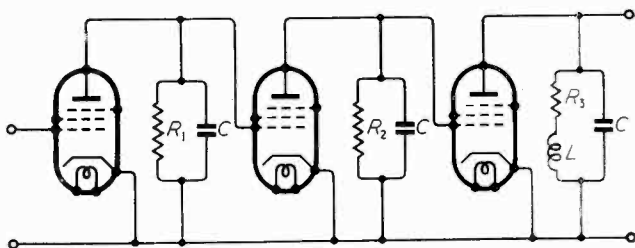


Fig. 5. Outline circuit and component values for amplifiers having the pole distributions of Fig. 1 and the frequency responses of Fig. 2.

	R_1	R_2	R_3	L
Landon	$\frac{1}{\omega_0 C}$	$\frac{1}{\omega_0 C}$	$\frac{1}{\omega_0 C}$	$\frac{1}{\omega_0^2 C}$
Linnebach	$1.5625 \frac{1}{\omega_0 C}$	$1.5625 \frac{1}{\omega_0 C}$	$0.4297 \frac{1}{\omega_0 C}$	$0.6713 \frac{1}{\omega_0^2 C}$

stages and this must be chosen to suit the distribution of energy in the frequency band to be amplified; and second, large values of n may lead to impossibly high Q -values for the inductors.

5. Acknowledgment

The author is indebted to the Engineer-in-Chief, G.P.O., for permission to publish this work.

REFERENCES

- ¹ Dietzold, R. L., "Network Theory comes of Age," *Elect. Eng.*, Sept. 1948.
- ² Linnebach, A., "Mehrkreisige Siebschaltungen mit ausgeglichener Resonanzkurve," *E.N.T.*, Oct. 1943.
- ³ Landon, V. D., "Cascade Amplifiers with Maximal Flatness," Parts I and II, *R.C.A. Review*, Jan. and April 1941.

DETUNED RESONANT CIRCUITS

Transient Response and S/N Ratio

By Herbert Elger, Dipl.Ing.

SUMMARY.—A simple way of calculating or graphically tracing the transients in detuned resonant circuits is shown in connection with a simple memory rule. Reference is made to the application of the method to similar mechanical and supersonic problems. The real response of resonant circuits when using pulse modulation or any other kind of shock excitation (such as static), the change of time constant due to detuning, and the signal-to-noise ratio are considered, and universal diagrams are presented.

THE problem of transients in oscillatory circuits is of increasing importance due to the growing use of pulse modulation for the most diverse purposes not only in electrical apparatus but also in mechanical and supersonic systems. In the following it will be shown that even the comparatively intricate transients occurring in detuned resonant circuits can be computed or constructed without the aid of anything but a simple memory rule. It will furthermore be shown that these 'detuned' transients are of great importance in static and short-pulse systems particularly with regard to the signal-to-noise ratio.

The most frequently occurring problem relates to the simple LC circuit comprising only linear elements and not coupled to any other circuit. It can readily be shown that there is no important or essential difference between a lumped LC circuit and any other type of simple resonant circuit such as distributed resonant circuits or resonant cavities. The theory developed in this paper may, however, in conjunction with the conventional coupled-circuit theorem, be applied also to more complicated networks, generally in the same way as to the continuously-oscillating or steady state.

The theoretical development of transients in simple circuits is a very lengthy procedure and will not, therefore, be treated here.^{1,2,3} The method adopted is derived differently, and one possibility is illustrated by the following (simplified) example. At the instant of connecting a parallel LC combination to an a.c. source, the reactance of the capacitor is zero and that of the coil infinite since the magnetic field has to be built up. Thus, the capacitor will charge almost instantaneously and discharge in an oscillatory manner through the coil. The current thus

consists of a constant alternating current of the supply frequency and a superimposed transient alternating current of the natural frequency of the circuit. The transient diminishes exponentially. When the supply voltage is disconnected, there is another transient identical with the above transient component of natural frequency but now, of course, independent of any difference between the initially applied frequency and the natural frequency of the circuit. Only in the case of two coupled resonant circuits mutually detuned will there be transients approximately corresponding to those in the exciting instant of a single resonant circuit detuned with respect to the exciting frequency.

Taking into account all normal factors influencing the transients, including the phase position of the exciting voltage at the switching-on instant $t = 0$, the complex transient voltage can be considered as being composed of two components, an invariable steady-state component $E \sin \omega t$ on which is superimposed a transient voltage component e_t , ω being the exciting angular frequency, and E the amplitude of the voltage produced across the circuit. The steady-state voltage amplitude E is, as usual, dependent on the applied exciting voltage and the coefficient of coupling between the circuit in question and the supply source. Thus, in case of a very loose coupling, the steady-state amplitude E across the circuit may be derived from the usual universal resonance curve [Fig. 4, curve (a)] and, hence, in the case of resonance, the resonant value of E is equal to about Q times the exciting voltage. In the following, E_0 designates this resonant voltage amplitude.

The transient voltage component e_t , which decreases with time, can be computed by means of the equation

$$e_t = E \cos(\omega_0 t - \beta) \cdot \frac{e^{-\delta t}}{\omega_0 \sqrt{LC}} \sqrt{1 + \left(\frac{1}{\omega^2 LC} - 1\right) \cos^2(\phi + \psi) - \frac{\delta}{\omega} \sin 2(\phi + \psi)} \quad \dots \quad (1)$$

in which $\tan \phi = \frac{1}{\omega CR} - \frac{\omega L}{R} = Q \left(\frac{\omega_0}{\omega} - \frac{\omega}{\omega_0} \right)$

MS accepted by the Editor, February 1949

$$\tan \beta = \frac{\omega \omega_0 LC \tan(\phi + \psi)}{2Q \frac{(\frac{\omega}{\omega_0})^2 - 1}{(\frac{\omega}{\omega_0})^2 + 1}} \approx 2Q \frac{(\frac{\omega}{\omega_0})^2 - 1}{(\frac{\omega}{\omega_0})^2 + 1}$$

ψ = phase position of exciting voltage at $t = 0$

$\delta = \frac{R}{2L}$ = coefficient of damping

ω_0 = natural angular frequency of the circuit

ω = angular frequency of supply.

Equ. (1) has been previously developed³ in another form, and applies to most general cases; viz., for arbitrary values of all quantities involved. Particularly in power-current engineering the above equation is very useful for determining the peak voltages and currents obtained due to switching-on or breaking impedances.

If Equ. (1) is to be used at high frequencies and with oscillatory circuits, it can be considerably simplified. The angles ψ and β may be assumed equal to zero (not however the angle ϕ , which is an indirect measure of detuning). In most cases $Q \gg 1$ and approximately constant provided that $|\omega_0 - \omega| = \Delta\omega \ll \omega_0$; therefore $\omega_0 \approx 1/\sqrt{LC}$. Thus the simplified Equ. (1) yields total switching-on transient:

$$\frac{e}{E} = \sin \omega t - e^{-\omega_0 t/2Q} \sin \omega_0 t \quad \dots \quad (2a)$$

total switching-off transient:

$$\frac{e}{E} = e^{-\omega_0 t/2Q} \sin \omega_0 t \quad \dots \quad (2b)$$

and in case of resonance (i.e., $\omega = \omega_0$) we obtain from Equ. (2a) the well-known formula

$$\frac{e}{E} = (1 - e^{-\omega_0 t/2Q}) \sin \omega_0 t \quad \dots \quad (2c)$$

Switching-on and off corresponds to the front and rear edges respectively of an applied rectangular pulse. The negative polarity of the second term in Equ. (2a) indicates phase-opposition between the transient voltage component and the steady-state voltage component at the switching-on instant $t = 0$. The equations (2) show that any transient is over, in practice, after $t = 10 Q/\omega_0$ seconds at the latest; i.e., after this time $e = E \sin \omega t$ or, after a switching-off instant, $e = 0$.

When considering amplitudes only, sine and cosine functions of ωt and $\omega_0 t$ in final equations such as Eqs. (2b) and (2c) may be put equal to unity.

The ratio of voltage amplitudes to current amplitudes in oscillatory circuits of any kind is invariably identical with the characteristic impedance Z_0 of the circuit both with regard to

transients and continuous occurrences. Exactly the same applies to acoustic and mechanical oscillatory circuits,⁴ the electrical voltage corresponding to pressure or mechanical force, and the electrical current corresponding to air stream velocity or movement velocity; e.g., the movement velocity of an oscillating part of a tuning fork. The mechanical characteristic impedance, the resistance, the mechanical quality Q , etc., may thus be readily defined; e.g., Z_0 is the ratio of maximum force to maximum movement velocity independent of their individual absolute values. Similar considerations are likely to be applicable to quartz crystals, etc. All the following considerations can thus be transferred in a similar manner to corresponding non-electrical problems and have lately been used to investigate the performance of stone-drilling machines with rapidly reciprocating chisels.

At resonance the oscillatory circuit exhibits a delay feature identical with that of a common RC or RL network, its time constant being $\tau = 2Q/\omega_0$; therefore such a circuit may be used as a delay member or a saw-tooth modulating member.

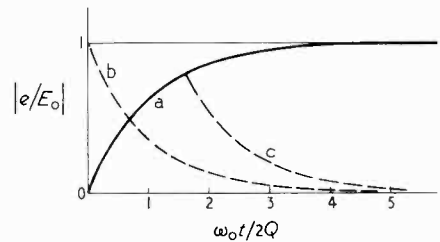


Fig. 1. Envelope transient response of resonant circuit tuned to the supply frequency; curve (a) switching on, curve (b) switching off, curve (c) pulse.

The transient response of a resonant circuit which is correctly tuned to the exciting frequency is shown in Fig. 1. Curve (a) represents the switching-on response, and curve (b) the switching-off response. Both curves are universal due to the scale chosen for the time-axis, and indicate the absolute value of the voltage (or current) amplitude across the circuit as a function of time, frequency and quality Q . Curve (c) shows an example of an 'incomplete' transient response derived by applying a short pulse of the duration $t = 1.6 \times 2Q/\omega_0$. In order to plot the complete transients as they would be shown on an oscilloscope screen it is necessary to complete the curves by their images on the other side of the time axis and by drawing radio-frequency oscillations between them as in the example of Fig. 3, which shows the complete transients of a detuned circuit. This pattern is well-known, more particularly, from carrier-wave telegraphy.

In the case of exciting a circuit with an off-resonance frequency, the difference between the natural and exciting frequencies being small, compared with either of them, the following formula is directly derived from Equ. (2a).

$$\frac{e}{E} = \sqrt{1 - 2e^{-\omega_0 t/2Q} \cos \Delta\omega t + (e^{-\omega_0 t/2Q})^2} \quad (3a)$$

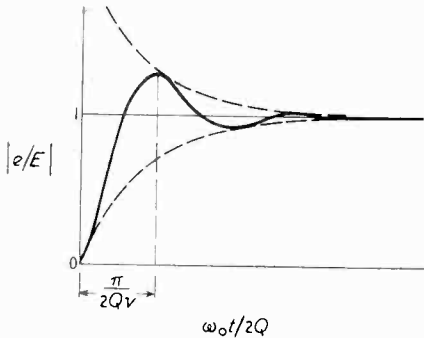


Fig. 2. Envelope transient response of a detuned circuit.

This equation yields the ratio of instantaneous voltage amplitude e (amplitude, since $\sin \omega t$ has been put equal to unity) to steady-state voltage amplitude E across the circuit or, in other words, it yields the envelope of the r.f. oscillations. In order to determine the desired maximum and minimum values and positions of the amplitude, the following approximation is quite sufficient.

$$\pm \frac{e}{E} = 1 - e^{-\omega_0 t/2Q} \cos \Delta\omega t \dots \dots (3b)$$

The envelope curve of 'detuned' transients thus exhibits a shape similar to a damped oscillation of the frequency $\Delta\omega$, the 'ripple' of the transient amplitude to a beat frequency. This is shown in Fig. 2. From Equ. (3) we obtain also the essential fact that it is possible to construct graphically the transient response of any resonant circuit tuned or detuned to any desired degree within not too wide limits. The four curves interconnecting the minima and maxima of the transient amplitudes on each side of the time axis (viz., the curves on which all maxima and minima must occur) are given by the four equations

$$\pm \frac{e}{E} = 1 \pm e^{-\omega_0 t/2Q} \dots \dots (3c)$$

the different polarity signs being entirely independent of each other. The transient crest amplitudes coincide with $\Delta\omega t = \pi, 3\pi, 5\pi \dots$ (odd multiples of π), the minimum amplitudes with even multiples of π , and the intersections of the amplitude envelope with the line $e/E = \pm 1$ coincide with odd multiples of $\pi/2$. The method

is shown in Fig. 3, the curves according to Equ. (3c) being plotted in dashed lines.

In order to plot any 'detuned' (or tuned) transients it is, therefore, only necessary to plot the four general e -functions and subdivide the time axis according to the beat frequency given by the difference between the exciting and natural frequencies; i.e., given by the degree of detuning. The course of the amplitude may then readily be traced manually. The first maximum amplitude is in practice the most important point, having a time delay of $1/(2\Delta f)$ with respect to time $t = 0$.

Contrary to the resonant case the transient peak amplitude in detuned circuits is *always* higher than the steady-state amplitude but lower than the steady-state amplitude of the same circuit when in resonance, provided that the exciting voltage is not varied. By excessive detuning it is possible to obtain peak amplitudes of nearly twice the steady-state amplitude, which can readily be shown on an oscilloscope by detuning a loosely-coupled secondary circuit of a pulse transmitter. In transmitter circuits, however, the exciting voltage is generally increased by detuning (usually causing a mismatch); e.g.,

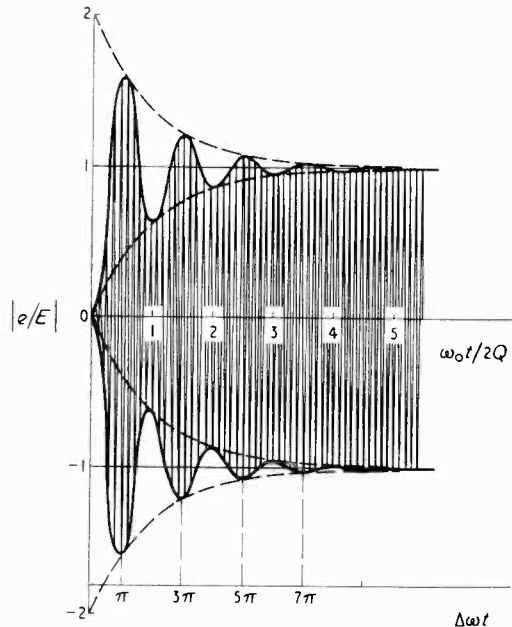


Fig. 3. Complete transient response of a detuned circuit.

if the aerial circuit is detuned with respect to the transmitter output. In this case any detuning may cause a considerable voltage rise, not only by mismatching, but also by the simultaneously increasing transient voltage peak. If the internal

resistance of the transmitter is considered as constant, the transient output voltage peak may become up to four times the tuned matched value. This fact is important for the design of high-power pulse transmitters, and also with regard to the time delay of ignition of t.r. valves in radar duplexers.

Due to transients a rectangular incident pulse can be reproduced neither faithfully nor symmetrically by a resonant circuit. Detuning the circuit makes possible, however, a decrease of the time constant and a much steeper reproduced pulse front and rear provided that a sufficient deviation from the midpoint of the resonance curve is chosen, although it is at the cost of the useful signal voltage when applied to receiver circuits. The ratio of the steady-state voltage of a detuned circuit to the resonance voltage of the same circuit correctly tuned is given by the resonance curve equation

$$\frac{E}{E_0} = \frac{1 - v}{\sqrt{1 + (2Qv)^2}} \quad \dots \quad (4)$$

In the numerator, the detuning factor $v = \Delta f/f_0$ is usually negligible. If only the conventional bandwidth has to be used, the permissible coefficient of detuning is $v_{max} = 1/(2Q)$; i.e., $(Qv)_{max} = 1/2$.

In receiver problems it is interesting to determine the relation between the maximum transient amplitude of a detuned circuit and the steady-state amplitude of the same circuit at resonance, the effective exciting voltage being unchanged. The maximum transient amplitude e_{max} is attained at $t = \pi/\Delta\omega$, and this inserted in Equ. (3a) gives

$$\frac{e_{max}}{E} = 1 + e^{-\pi/2Qv} \quad \dots \quad (5)$$

and, consequently, the desired relation may be obtained from Eqs. (5) and (4)

$$\frac{e_{max}}{E_0} = (1 - v) \frac{1 + e^{-\pi/2Qv}}{\sqrt{1 + (2Qv)^2}} \quad \dots \quad (6)$$

The performance of a resonant circuit is, thus, different when using pulse-modulated waves from that when applying continuous waves. Measurement with the aid of a pulse signal generator together with a high-resistance peak voltmeter gives, therefore, a resonance curve different from that obtained by using any other type of signal generator or voltmeter. Fig. 4 shows the two universal resonance curves in question. Curve (a) is the conventional resonance curve according to Equ. (4), and (b) the pulse resonance curve according to Equ. (6) provided that v is small with respect to unity. Curve (c) in Fig. 4 shows the percentage of the maximum transient amplitude rising above the steady-state ampli-

tude, all curves being plotted as a function of Qv and thus being universal. The two vertical lines indicate the bandwidth limits $Qv = 0.5$.

From the diagram it may be seen that there is a distinct difference in action between various kinds of interference in the r.f. input circuit of a receiver. Any shock excitation, such as by atmospherics, outside the bandwidth limits results in a much greater volume of reproduced noise than continuous interference of the same original strength; e.g., from an adjacent broadcast transmitter. Within the bandwidth this difference is substantially imperceptible. The difficulty of eliminating pulse interference by using high- Q resonant circuits is evident. As many types of short-pulse receiver act more or less as differentiating devices, not only the time constant but also the transient response may influence the reproduction. If the circuit is but slightly detuned as in Fig. 2 the differentiating action is improved since the pulse front transferred by the circuit to the

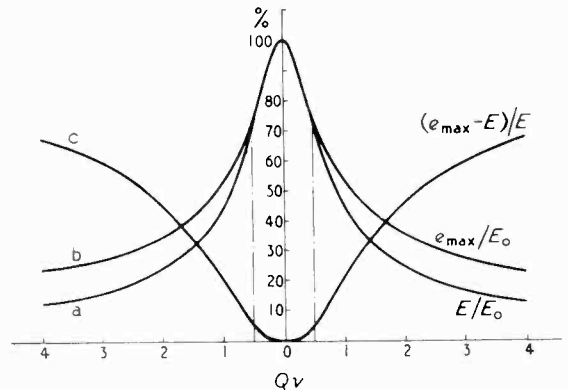


Fig. 4. Universal resonance curves; (a) is the steady state response and (b) the pulse response. Curve (c) shows the percentage of the maximum transient amplitude above the steady-state amplitude.

input valve or crystal becomes steeper, while the ripple of the transient is differentiated substantially without distortion. The time constant of the circuit decreases with increasing detuning. Assuming that $\omega_0 = 1,000$ Mc/s and $Q = 100$ (i.e., $\lambda = 1.88$ m and relative bandwidth = 1%), and assuming that it is desired to attain 90% of the steady-state voltage during a pulse, the time required with a resonant circuit is $0.46 \mu\text{sec}$. If the coefficient of detuning $v = 0.5\%$, that is 5 Mc/s off resonance, and thus $Qv = 0.5$, the time required for attaining 90% of the steady-state value is $0.22 \mu\text{sec}$, or less than half the time required at resonance. Detuning 0.5% corresponds in this case to a voltage drop of 30%, compared with resonance voltage, but if pulses shorter than $0.5 \mu\text{sec}$ have to be received it

would evidently be advantageous to detune the circuit (neglecting noise) in every case and, more particularly, in differentiating receivers.

In practice, the influence of noise cannot be generally treated here due to the different behaviour of internal and external noise when detuning. A simple example will show the signal-to-noise ratio of a closed quarter-wavelength-resonant circuit. Similar results are also obtained with resonant circuits of any other type, and the qualitative results will always be the same.

The impedance of a closed line is $Z = Z_0 \tanh(a + jb)$ and its resistance $R = Z_0(1 + \tan^2 b)/(1 + \tan^2 b \tanh^2 a)$. Provided that the detuning v is less than 15% (i.e. that $\tan v \approx v$), $Q \gg 1$ and the length of the resonant line is $\lambda/4$, we obtain the resistive component

$$R \approx \frac{Z_0}{\pi Q} \cdot \frac{1 - v}{v^2 + 1/4Q^2} \quad \dots \quad (7)$$

If B designates the absolute bandwidth, the r.m.s. noise voltage E_n becomes

$$E_n^2 = 4kTBR = 4kTR \frac{f_0}{Q} \\ = 4kT \frac{f_0 Z_0}{\pi Q^2} \cdot \frac{1 - v}{v^2 + 1/4Q^2} \quad \dots \quad (8)$$

The signal-to-noise ratio S/N related to maximum transient amplitude can thus be derived from Eqs. (6) and (8), the resonant voltage E_0 being replaced by the product of exciting voltage and Q .

$$\frac{S}{N} = Q \frac{1 + e^{-\pi/2Qv}}{\sqrt{16kTf_0 Z_0}} \approx Q \frac{1 + e^{-\pi/2Qv}}{\sqrt{5.10kTf_0 Z_0}} \quad (9a)$$

By detuning up to the bandwidth limit $Qv = 0.5$ the signal-to-noise ratio becomes

$$\frac{S}{N} = \frac{1.04Q}{\sqrt{5.10kTf_0 Z_0}} \quad \dots \quad (9b)$$

From the above formulae it will be seen that the signal-to-noise ratio is approximately independent of detuning in the region of the bandwidth unless certain external noise sources, such as valve noise, are not negligible compared with the thermal noise of the circuit. On the other hand, noise produced by external resistances coupled with the circuit considered will not produce any change of the ratio according to Equ. (9) when the actual effective Q of the complex combination is inserted, and unless Q is substantially varied by detuning.

The importance of the above calculations may again be shown by an example. We assume again that $Q = 100$, permissible detuning $v = 0.005 = 0.5\%$ and resonance resistance 5000 ohms (or more). The effective resistance of the circuit

detuned up to the bandwidth limit is then 1000 ohms (or more). To this resistance has to be added the equivalent grid-noise resistance of the subsequent valve, and its gain is assumed to be such as to make the reflected load resistance of the valve negligible; i.e., in this case less than about 50 ohms. If the noise resistance of the valve is sufficiently low, say, some hundreds of ohms, the signal-to-noise ratio of the complete input stage is not changed to any great extent by detuning. The time constant is, however, considerably less than in the resonant case, the effect of a subsequent differentiating stage being noticeably improved, and consequently the sensitivity of the receiver enhanced. It may, however, be noted that a deterioration is to be expected with respect to incident pulses in the vicinity of or below the noise level.

Finally, it may be mentioned that during the war experiments were made to suppress 'window' interference in radar receivers by using extremely short pulses or pulse groups—so-called comb pulses. It has been supposed that the time constant of large targets reflecting incident pulses is almost zero or, in any case, considerably less than that of the resonant windows. The fronts of the pulses reflected from the resonant windows were assumed to be inclined, due to the greater time constant. By inserting high- Q resonant circuits across the receiver line in such a manner that these circuits are insulating during their transient time only, it was expected that only the front part of a pulse would be passed through the line to the receiver input. Pulses having perceptibly inclined fronts would thus be separated and suppressed since the resonant filter circuit would act as a nearly perfect short-circuit after about $8Q/\omega_0$ seconds. The desired effect was supposed to be improved by subsequent differentiating. The experiments were, however, entirely unsuccessful, and this has been proved by the author also theoretically, since slightly detuned windows reflect pulses with a much shorter time constant, though with smaller amplitude. Furthermore, resonant filter circuits having a sufficient time constant, and consequently high Q , are extremely sensitive in their transient response to any detuning, as Qv must be quite negligible in order not to reduce the time constant of the filter unduly.

REFERENCES

- ¹ J. G. Brainerd, "Ultra-high-Frequency Techniques," page 367, D. van Nostrand Co. Inc.
- ² A. W. Glazier, "Transient Response of Symmetrical 4-terminal Networks," *Wireless Engineer*, 1948, Vol. 25, p. 6.
- ³ A. Fraenckel, "Theorie der Wechselströme," Julius Springer (1930)
- ⁴ K. W. Wagner, "Einführung in die Lehre von den Schwingungen und Wellen." Friedrich Klemm (1947).

TWO-CAVITY KLYSTRON

Effect of Space Charge

By Bernard Meltzer

(Development Department, Mullard Radio Valve Co., Ltd., Mitcham, Surrey)

Introduction

WEBSTER'S¹ original paper on velocity modulation not only solved the problem of kinematic bunching (i.e., the bunching that would take place if no space-charge forces acted on electrons in the drift space) but also attacked in an approximate manner the problem of the effect of space charge. However, his argument in the latter connection was never quite clear and it is worth while to examine the question from a somewhat more fundamental point of view; especially since klystrons are today being developed to a greater extent as power generators, and not merely as local oscillators with relatively low space-charge densities. It is true that British workers² in this field have stated that the Webster type of analysis enormously over-estimates the effect of space charge, because by its assumption of a beam of infinite cross-section it ignores the effect of the bounding wall of the drift space. The evidence for this judgment does not appear to have been published; but even if it is true, the analysis of conditions inside an infinite beam will still be of value because it will give approximately correct results for the centre of the beam in the case of distant bounding walls, and because it is the simplest analysis of the space-charge problem.

In this paper, the two fundamental differential equations governing electron flow in the drift space are obtained. These are valid only while the motion preserves its single-stream character, and the analysis itself predicts when this condition ceases to hold; i.e., when overtaking occurs. It is assumed that thermal variations of velocity may be ignored, and that particle speeds are so low that the forces due to the magnetic field of the current may be ignored. Rationalized m.k.s. units³ are used.

General Analysis

Since a beam of infinite cross-section flowing in one direction is being considered, the electric field in the beam is wholly in the direction of flow. Let the electron which entered the drift space at time t_1 have travelled a distance s by time t , so that we have

$$s = s(t, t_1) \quad \dots \quad (1)$$

This function is the basic function employed. It should be noted that, unless otherwise indicated, all the partial differential coefficients used are with respect to t or t_1 constant.

Let the electric field E existing at s at time t be given by

$$E = E(s, t) \quad \dots \quad (2)$$

The equation of motion of the electron is

$$(d/dt)v = -\eta E(s, t) \quad \dots \quad (3)$$

where

v = speed of electron, and

$\eta = (e/m)$ for an electron.

As the electron moves, the field moving it changes in general both because the position of the electron is changing and because time is advancing. Hence, from (3),

$$(d/dt)(dv/dt) = -\eta[(\partial E/\partial s)_t v + (\partial E/\partial t)_s] \quad \dots \quad (4)$$

Now, by Poisson's Law,

$$(\partial E/\partial s)_t = (\epsilon/\epsilon_0)\rho \quad \dots \quad (5)$$

where

ϵ_0 = permittivity of free space, and

$\rho = \rho(s, t)$ = charge density.

Hence equation (4) becomes

$$(d^2v/dt^2) = -\eta[(\epsilon/\epsilon_0)\rho v + (\partial E/\partial t)_s] \quad \dots \quad (6)$$

ρv equals the conduction current density at s , and $\epsilon_0(\partial E/\partial t)_s$ equals the displacement current density. Hence equation (6) becomes

$$(d^2v/dt^2) = -\eta I/\epsilon_0 \quad \dots \quad (7)$$

where

I = total current density at $s = s$.

It is to be noted that this is the point at which the single-stream assumption is first made. For the general case one would have

$$I = \rho_1 v_1 + \rho_2 v_2 + \dots + \epsilon_0 (\partial E/\partial t)_s \quad (8)$$

where the suffices refer to the different streams.

Equation (7) may be rewritten

$$(\partial^3 s/\partial t^3) = -(\eta/\epsilon_0)I(t) \quad \dots \quad (9)$$

the partial differentiation sign being used, because s is also a function of t_1 . The right-hand side of equation (9) is positive because the current is electronic.

We now proceed to obtain the second fundamental differential equation, namely,

MS accepted by the Editor, February 1949

$$(\partial^3 s / \partial t_1 \partial t^2) = (\eta / \mathcal{E}_0) I_0(t_1) \quad \dots \quad (10)$$

where

$I_0(t_1)$ = electron current entering at $s = 0$; we will incidentally obtain explicit expressions for conduction current density, charge density, electric field, voltage, and condition for overtaking, in terms of the function

$$s = s(t, t_1)$$

which is the integral of equations (9) and (10).

If I_c = electronic current as $s = s$,

it follows, since charge is conserved, that

$$I_0(t_1) dt_1 = I_c dt \quad \dots \quad (11)$$

where dt represents the time taken to cross the $s = s$ plane by the set of electrons which, previously, took time dt_1 to enter the drift space, so that

$$dt_1 = (\partial t_1 / \partial t)_s \cdot dt$$

$$\text{Hence } I_c = I_0(t_1) (\partial t_1 / \partial t)_s \quad \dots \quad (12)$$

and there is no need to enclose

$$(\partial t_1 / \partial t)_s$$

in modulus bars, because it is positive in the absence of overtaking.

Now, from equation (1),

$$(\partial t_1 / \partial t)_s = - (\partial s / \partial t) / (\partial s / \partial t_1) \quad \dots \quad (13)$$

Therefore,

$$I_c = - I_0(t_1) (\partial s / \partial t) / (\partial s / \partial t_1) \quad \dots \quad (14)$$

But

$$\rho = I_c / (\partial s / \partial t)$$

$$\text{therefore } \rho = - I_0(t_1) / (\partial s / \partial t_1) \quad \dots \quad (15)$$

From equation (5), ρ is also given by

$$\begin{aligned} \rho &= \mathcal{E}_0 (\partial E / \partial s)_t \\ &= \mathcal{E}_0 (\partial E / \partial t_1)_t / (\partial s / \partial t_1)_t \quad \dots \quad (16) \end{aligned}$$

Equating equations (15) and (16) gives

$$\mathcal{E}_0 (\partial E / \partial t_1)_t = - I_0(t_1) \quad \dots \quad (17)$$

From equation (3),

$$E = - (1/\eta) (\partial^2 s / \partial t^2) \quad \dots \quad (18)$$

substituting this in equation (17) gives equation (10) presented above, namely,

$$(\partial^3 s / \partial t_1 \partial t^2) = (\eta / \mathcal{E}_0) I_0(t_1) \quad \dots \quad (10)$$

Explicit expressions for charge density and field at any point are given by equations (15) and (18).

The voltage V between $s = 0$ and $s = s$ is obtained as the integral

$$V = - \int_0^s E(s, t) ds \quad \dots \quad (19)$$

where t is kept constant in the integration, s and t_1 being varied.

Substituting from equation (18) gives

$$V = (1/\eta) \int_0^s (\partial^2 s / \partial t^2) ds \quad \dots \quad (20)$$

(t constant in integration),

or

$$\begin{aligned} V &= (1/\eta) \int_t^{t_1} (\partial^2 s / \partial t^2) (\partial s / \partial t_1) dt_1 \\ &= - (1/\eta) \int_{t_1}^t (\partial^2 s / \partial t^2) (\partial s / \partial t_1) dt_1 \quad \dots \quad (21) \end{aligned}$$

(t constant in integration),

The condition for overtaking is clearly

$$(\partial t / \partial t_1)_s = 0 \quad \dots \quad (22)$$

i.e., from equation (13),

$$(\partial s / \partial t_1) = 0 \quad \dots \quad (23)$$

Discussion and Integration of Equations

The results obtained in the last section are quite general for one-dimensional rectilinear flow. For example, they apply to the case of a plane diode, where the drift space is now the cathode-anode space, and $s = 0$ and $s = s$ represent respectively the cathode and anode planes.

The results are two-fold; first, it has been shown that the electron motion is governed by the following two differential equations:

$$(\partial^2 s / \partial t^2) = - (\eta / \mathcal{E}_0) I(t) \quad \dots \quad (9)$$

$$(\partial^3 s / \partial t_1 \partial t^2) = (\eta / \mathcal{E}_0) I_0(t_1) \quad \dots \quad (10)$$

where

$I(t)$ = total current density (electronic plus displacement) in the beam, and $I_0(t_1)$ = electron-current density at entry; secondly, once these equations have been integrated, use can be made of the explicit expressions of equations (14), (15), (18), (21) and (23) to obtain, respectively, conduction current density, charge density, electric field, voltage at any point in the beam, and the condition for overtaking.

First, we proceed to integrate the equations of motion and note that it is better to start with equation (10) than with equation (9), since in most applications $I_0(t_1)$ is a known constant, if one neglects the small density modulation imposed by the buncher, while $I(t)$ is usually not known a priori.

Let the velocities imposed by the buncher on the electrons at entry be given by $v(t_1)$ and let the acceleration of the electrons on entry be $a(t_1)$. In any particular problem $v(t_1)$ is known, while $a(t_1)$ —as will be seen below—depends on the klystron model one assumes.

Integrating equation (10) with respect to t_1 , gives

$$(\partial^2 s / \partial t^2) = \sigma(t - t_1) + a(t) \quad \dots \quad (24)$$

where σ is a positive constant given by

$$\sigma = - (\eta / \mathcal{E}_0) I_0$$

Integrating equation (24), with respect to t , twice gives

$$(\partial s/\partial t) = v(t_1) + (\sigma/2)(t - t_1)^2 + \int_{t_1}^t a(\theta)d\theta \quad (25)$$

and, finally,

$$s = v(t_1)(t - t_1) + (\sigma/6)(t - t_1)^3 + \int_{t_1}^t d\phi \int_{t_1}^{\phi} a(\theta)d\theta \quad (26)$$

where θ and ϕ are integration variables.

Equation (9) may now be used to give the total current density $I(t)$:

$$I(t) = I_0 - (\mathcal{E}_0/\eta)(d/dt) a(t) \quad (27)$$

Applications

1. Plane Diode

The results for this case, though well-known, are worked out here, because they will be needed for the second klystron model used later, and to show a simple application of the somewhat unfamiliar formulae above.

For a plane diode in the space-charge-limited régime

$$v(t_1) = 0, \text{ and}$$

$$a(t_1) = 0,$$

the latter equation holding because the electric field is zero at the cathode.

The equation of motion (26) becomes

$$s = (\sigma/6)(t - t_1)^3$$

The total current density $I(t)$ is given by equation (27): $I(t) = I_0$.

The conduction current density is, of course, the same constant.

The charge density follows from equation (15):

$$\rho = 2I_0/\sigma(t - t_1)^2 \\ = -(\sqrt[3]{6}/3)(\mathcal{E}_0/\eta)^{1/3}(I_0/s)^{2/3}$$

The electric field is given by equation (18):

$$E = (I_0/\mathcal{E}_0)(t - t_1) \\ = -(\sqrt[3]{6})(I/\mathcal{E}_0)^{2/3}(I/\eta)^{1/3}I_0^{2/3}s^{1/3}$$

The cathode-anode potential difference is given by equation (21):

$$V = (I/\eta)(\sigma/2) \int_{t_1}^t (t - t_1)^3 dt_1$$

(t constant in integration)

$$= (3\sqrt[3]{6}/4)(I/\mathcal{E}_0)^{2/3}(I/\eta)^{2/3}I_0^{2/3}s^{4/3}$$

We shall need below the value of the acceleration at the plane $s = s_0$. From the expression for electric field it is given by

$$a_0 = (\sqrt[3]{6})(\eta/\mathcal{E}_0)^{2/3}I_0^{2/3}s_0^{1/3} \quad (28)$$

2. Drift-space of Klystron: Zero Initial Acceleration

We assume that the electrons enter the drift space with a velocity modulation imposed by the buncher, given by $v(t_1)$, and in a region of zero field, and therefore, with zero initial acceleration.

The latter assumption makes this an unreal

model (Fig. 1): for at the entry plane there will in general be a finite electric field due to the electrons in the drift space, to the induced charges on the buncher and catcher walls at the two ends of the drift space and to the electrons in the beam outside the drift space. Nevertheless, we shall treat it as if it were a valid model, comparing results with those of Webster's kinematical model (which of course implicitly makes the same assumption); for the resulting simple analysis can be taken over

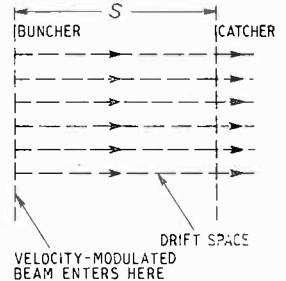


Fig. 1. Case of a klystron with zero initial acceleration.

with simple modifications into the theory of the second model developed later.

For this case, it follows from equation (26) that

$$s - v_1(t_1)(t - t_1) = (\sigma/6)(t - t_1)^3 \quad (29)$$

Webster's kinematical theory is based on the assumption that the right-hand side of equation (29) is negligible.

We proceed to obtain the condition for the 'correctness' of kinematical theory. We must have

$$(\sigma/6)(t - t_1)^3 \ll v_1(t - t_1)$$

At the same time, we have, approximately,

$$s = v_1(t - t_1)$$

Therefore the condition is

$$(\sigma/6v_1^3)s^2 \ll 1$$

or

$$(\eta/6\mathcal{E}_0)|I_0|(I/v_1^3)s^2 \ll 1 \quad (30)$$

If, instead of v_1 , we write the average speed v_0 of the electrons at entry, we have

$$(\eta/6\mathcal{E}_0)|I_0|(I/v_0^3)s^2 \ll 1 \quad (31)$$

Except for the factor 6 (which may be important in border-line cases of moderately-high current densities), this is the same as the condition that Webster obtained.

If we translate equation (31) into transit-angle terms, we have

$$(I/24\pi^2)(I/\mathcal{E}_0)(\eta/2)^{1/2}|I_0|V_0^{1/2}(I/f^2)\phi^2 \ll 1 \quad (32)$$

where

$$\phi = \text{d.c. transit angle of drift-space,}$$

V_0 = steady accelerating voltage of klystron, and f = frequency of modulation.

Applying equation (32) to the particular case of a 6-cm, 500-V, 100-mA klystron with beam-cross-section 0.5 sq cm, gives

$$\phi \ll 14 \text{ approx.}$$

Now for maximum power output at the catcher for the small-signal kinematical case, Webster showed that

$$(1/2) \alpha \phi = 1.84$$

where

$$\alpha = \text{modulation factor at buncher.}$$

Even if $\alpha = 1$ (actually precluded by the small-signal assumption), this means that ϕ is approximately 25% of 1.4. If, as is more to the point, $\alpha = 1/10$, ϕ will be more than twice 1.4. Thus kinematical theory would be hardly applicable, and bunching would have to be studied on the basis of equation (29), after the particular velocity modulation imposed has been substituted for $v_1(t_1)$ in it.

Bunching in Drift-space

From equation (29) it follows that

$$\left(\frac{ds}{dt_1}\right) = \left(\frac{dv_1}{dt_1}\right)(t - t_1) - v_1 - \frac{(\sigma/2)(t - t_1)^2}{\dots} \dots \dots (33)$$

and

$$\left(\frac{ds}{dt}\right) = v_1 + (\sigma/2)(t - t_1)^2 \dots \dots (34)$$

Therefore, from equation (14), the conduction current density is given by

$$I_c = I_0 \frac{v_1 + (\sigma/2)(t - t_1)^2}{v_1 + (\sigma/2)(t - t_1)^2 - \left(\frac{dv_1}{dt_1}\right)(t - t_1)} (35)$$

To obtain full information about the Fourier components of the current in any particular problem, it would be necessary to solve equation (29) for t_1 and substitute in equation (35).

But in this note we shall limit ourselves to pointing out one new general result following from equation (35), which distinguishes space-charge bunching from kinematical bunching.

Overtaking can take place only if the denominator of equation (35) can become zero. This first occurs when

$$t - t_1 = \frac{(1/\sigma)\left(\frac{dv_1}{dt_1}\right) - \left\{\left(1/\sigma\right)^2\left(\frac{dv_1}{dt_1}\right)^2 - \left(2v_1/\sigma\right)\right\}^{1/2}}{\dots} \dots \dots (36)$$

Therefore, for overtaking to be possible,

$$(1/\sigma)^2 \left(\frac{dv_1}{dt_1}\right)^2 \geq (2v_1/\sigma) \dots \dots (37)$$

Furthermore, (dv_1/dt_1) , must clearly, be positive; hence condition (37) becomes

$$\left(\frac{dv_1}{dt_1}\right) \geq (2\sigma v_1)^{1/2} \dots \dots (38)$$

or, more perspicuously,

$$\left(\frac{d}{dt_1}\right) \sqrt{v_1} \geq \sqrt{\sigma/2} \dots \dots (39)$$

This lays down a lower limit for the rate of velocity modulation required to produce overtaking.

If this is applied to the small-signal case, where the velocity modulation is given by

$$v_1 = \{(2\eta V_0)^{1/2}\} \{1 + (\alpha/2) \sin 2\pi f t_1\}$$

α , V , f representing respectively the buncher

modulation factor, steady voltage and frequency of the klystron, one obtains approximately

$$\alpha \geq (1/\pi f)(2\eta V_0)^{1/4} (|I_0|/\mathcal{E}_0)^{1/2} \dots \dots (40)$$

Applying this to the previously considered example gives

$$\alpha \geq 0.16$$

According to kinematical theory, on the other hand, overtaking will always take place, provided the drift space is sufficiently long.

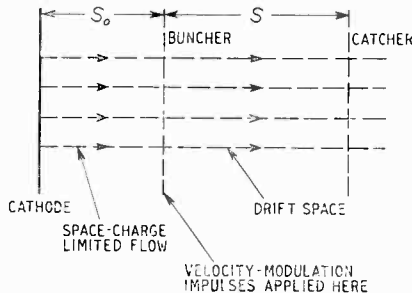


Fig. 2. Case of a klystron with finite initial acceleration.

3. Klystron with Space-charge-limited Cathode

In this model (Fig. 2), it is assumed that the beam emerges from a space-charge-limited plane cathode and, at a plane distant s_0 from the cathode, impulses are given to the electrons (by a 'ghost' buncher), which impose the given velocity modulation $v(t_1)$ upon the beam. Distances s are measured from this plane.

This model is still imperfect in that it still excludes the buncher and catcher walls from the picture, but nevertheless it is probably closer to reality than the previous model, since—because of heat transfer troubles—most modern klystrons do not have grids across their buncher cavity apertures.

The initial acceleration $a(t_1)$ in this case is given by $a(t_1) = a_0$ where a_0 is the constant given by equation (28).

The equation of motion (26) now becomes

$$s - v_1(t_1)(t - t_1) = \frac{(\sigma/6)(t - t_1)^3}{(t - t_1)^2} + (a_0/2) \dots \dots (41)$$

In addition to the condition found for the previous model (equation 31), the correctness of Webster's analysis now also would require

$$(a_0/2)(t - t_1)^2 \ll s$$

Again putting

$$s = v_0(t - t_1) \text{ approximately,}$$

and using equation (28) and the value of the average entrance velocity v_0 given by the diode theory, one obtains

$$s \ll 3s_0 \dots \dots (42)$$

Thus the drift length would have to be considerably less than three times the cathode-to-buncher distance.

The expression (35) for the conduction current holds again except for the addition of the term $a_0(t - t_1)$ in numerator and denominator, so that the conduction current density is given by

$$I_c = I_0 \frac{v_1 + (\sigma/2)(t - t_1)^2 + a_0(t - t_1)}{v_1 + (\sigma/2)(t - t_1)^2 - \{(dv_1/dt_1) - a_0\}(t - t_1)} \quad (43)$$

Hence the condition for the possibility of overtaking is a slight formal modification of equation (38), namely,

$$(dv_1/dt_1) - a_0 \geq (2\sigma v_1)^{1/2}$$

It is easy to check that actually, if we substitute for v_1 its average value v_0 , this condition reduces to

$$(dv_1/dt_1) \geq 2a_0 \quad (44)$$

Hence, at least in the small-signal case, only electrons which are modulated by the buncher at a rate greater than twice the acceleration they had on entering the buncher, will be in a position to overtake.

Finally it may be noticed that in both the above models, the total current density is constant, as appears from equation (27).

Acknowledgment

The writer wishes to thank Mrs. Berz of the Vacuum Physics Laboratory, Mullard Radio Valve Co., Ltd., for a discussion which led to a revision of this paper.

REFERENCES

- ¹ Webster, D. L.; *J. appl. Phys.*, 1939, Vol. 10, p. 301.
- ² Frenlin, J. H., Gent, A. W., Petrie, D. P. R., Wallis, P. J., Tomlin S. G.; *J. Instn elect. Engrs*, 1946, Vol. 93 Pt. IIIA, No. 5, p. 877.
- ³ Stratton, J. A.; "Electromagnetic Theory," McGraw-Hill, p. 16.

BOOK REVIEWS

Reference Data for Radio Engineers (Third Edition).

1 p. 672. Published by Federal Telephone and Radio Corporation, 67 Broad Street, New York 4. Price \$3.75.

This has twice as many pages as the second edition, but owing to the thinness of the paper is very little bigger or heavier. The first edition appeared in 1943. It has been compiled by engineers of the companies associated with the International Telephone and Telegraph Corporation. Much of the material of the second edition has been revised and expanded and many new chapters have been added. Chapter I on frequency data has been completely revised in accordance with the decisions made at the 1947 Atlantic City conference. Chapter 2 is on units, constants, and conversion factors; in it we are told that to convert leagues to miles one must multiply by 2.635; a little calculation shows that instead of taking the nautical mile as 1.15 statute miles they have reversed the figures. This gives one an uneasy feeling and suggests that one should check the data given before using it. Subsequent chapters deal with properties of materials, radio components, fundamentals of networks, selective circuits, filter networks, attenuators, bridges and impedance measurements, rectifiers and filters, iron-core transformers and reactors, electron tubes, amplifiers and oscillators, modulation, Fourier waveform analysis, transmission lines, waveguides and resonators, antennas, radio-wave propagation, radio noise and interference, radar fundamentals, broadcasting, wire transmission, electroacoustics, servo mechanisms, miscellaneous data, Maxwell's equations, mathematical formulas and tables.

There are a great number of graphs and diagrams and a 29-page index.

The dielectric constant and loss factor of 130 insulating materials are given for six frequency ranges. The chapter on valves includes travelling-wave, magnetron, and klystron tubes. The mathematical tables will prove very useful; they include all the trigonometrical and logarithmic tables, many pages of standard integrals and Laplace transforms.

The book provides over six hundred pages packed with useful information on all branches of radio.

G. W. O. H.

The Presentation of Technical Information

By REGINALD O. KAPP, B.Sc. (Eng.), M.I.E.E. Pp. 147 + xi. Constable & Co., Ltd., 10, Orange St., London, W.C.2. Price 6s.

This little book is based on four lectures given at University College, London and is worth the attention of all concerned with scientific literature, from the works report to the text book. The author is concerned with Functional English by which he means 'the English that any writer uses who expresses his meaning clearly and without ambiguity; who spares his readers unnecessary effort; who selects every item and places every sentence and every word so that it will meet the function assigned to it.' The purpose of Functional English 'is always to convey new information.'

The author stresses the importance of maintaining the receptivity of the reader and he points out that it is as necessary to present facts and statements in a correctly regulated flow as it is for a music-hall comedian to time the steps and climax of his story. If the style is too concise and fact follows fact without pause, the reader cannot assimilate them as he reads and he misses many of them. On the other hand, if the style is verbose the reader loses interest and receptivity and again does not readily absorb the facts.

Much of the book consists of amplification of these statements together with a discussion of ways in which the two extremes can be avoided. There is much sound common sense in it and few will quarrel with the author's view that the purpose of writing is not merely to set down information on paper but to convey it to the mind of the reader—a very different and much more difficult thing.

W. T. C.

Accumulator Charging (10th Edition)

By W. S. IBBETSON, B.Sc., A.M.I.E.E., M.I.Mar.E. Pp. 193 + xii. Sir Isaac Pitman & Sons Ltd., Parker St., Kingsway, London, W.C.2. Price 10s.

The Electronic Musical Instruments Manual

By ALAN DOUGLAS. Pp. 141 + vii. Sir Isaac Pitman & Sons Ltd., Parker St., Kingsway, London, W.C.2. Price 18s.

RADIOLYMPIA 1949

The 16th National Radio Exhibition

ALTHOUGH radio apparatus of all kinds was displayed at the exhibition, pride of place was given to television and few receiver manufacturers did not show a range of television sets. Projection models were shown for the first time by quite a large number of firms. These sets are based on the Mullard system using a 2½-in cathode-ray tube operating at 25 kV and providing a picture about 15 in by 12 in. The picture size is, of course, dependent on the magnification of the optical system and varies slightly in the different models.

The tube faces a spherical glass mirror of about 6-in diameter from which the light rays are reflected back towards the tube on to an inclined plane mirror which reflects the light again so that it passes out normal to the axis of the tube. This inclined mirror has a hole in its centre through which the tube passes. A corrector plate is mounted alongside the assembly in the path of the light from the inclined mirror to correct for the spherical aberration of the spherical mirror. This plate is manufactured by a gelatine moulding process.

The tube with its deflector and focus coils, the spherical and plane mirrors and the corrector plate form a sub-

assembly. The light emerging from the corrector plate falls on the rear of a flat viewing screen which is usually of a plastic material. Variations exist here between the different receivers, since for convenience in design, mirrors may be interposed between the viewing screen and the corrector plate.

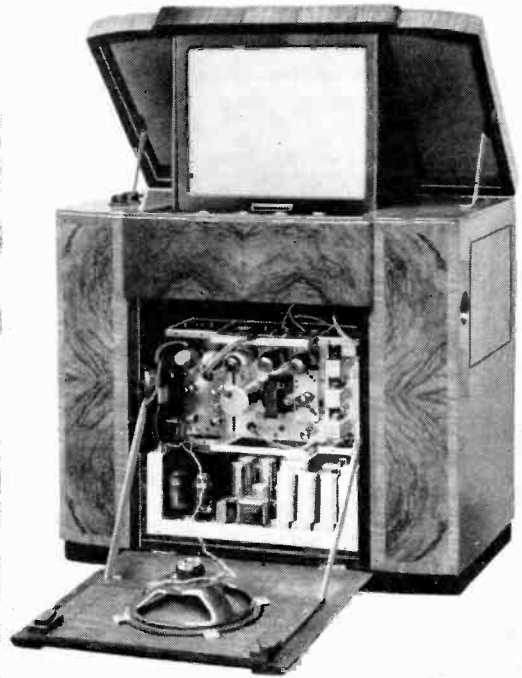
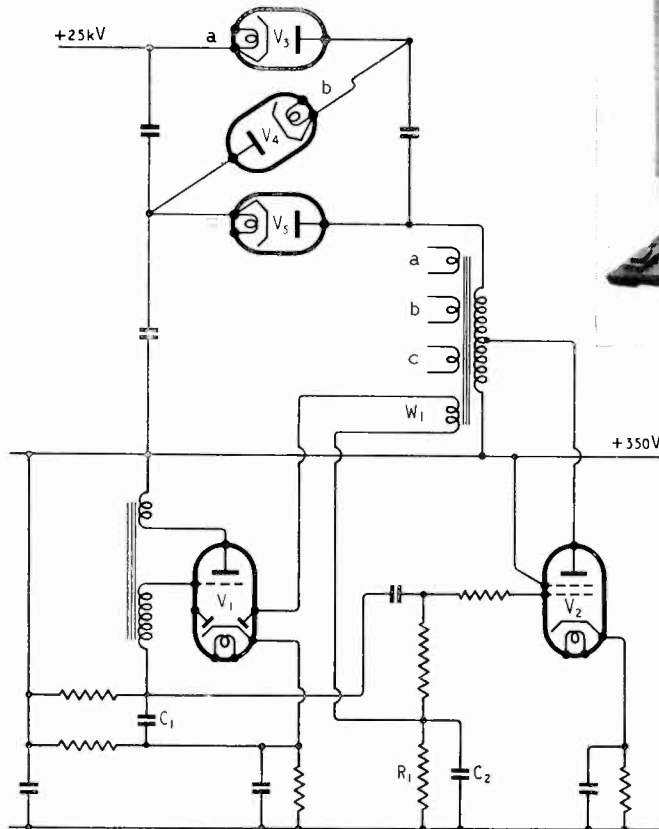


Fig. 1 (left). Circuit of typical 25-kV e.h.t. supply used in projection television sets.

(Above). R.G.D. projection television receiver with front dropped for access to the chassis.



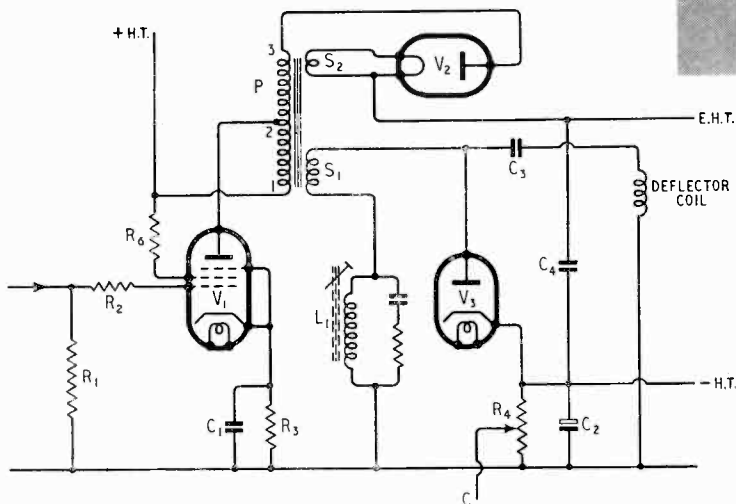
In some sets the screen is fixed in position, in others it is arranged to fold out of sight when the set is not in use. Thus, in the R.G.D. set the viewing screen is hinged at its top towards the front end of the lift-up lid of the cabinet.

The structure of the screen is arranged to give a much greater viewing angle in the horizontal plane than in the vertical, and to reduce the visibility of the scanning lines some form of line-broadening technique is adopted. Sometimes this is achieved by arranging for the

screen to give more diffusion vertically than horizontally, in others the scanning 'spot' is arranged to be a vertical line. It was noteworthy in the demonstrations that the line structure of the picture was much less evident than in the ordinary 12-in directly-viewed models. The picture brightness was considerably less, but quite adequate for viewing in semi-darkness and the definition was really good.

In spite of the high operating voltage the scanning power required is not large; in fact, it is stated to be rather less than is needed for conventional 9-in and 12-in tubes. The reason is that the deflection angle needed is less because of the greater length of the projection tube relative to its diameter.

The e.h.t. supply is obtained from a source of some 9 kV through a voltage-tripler rectifier system using hard valves. The 9-kV source is itself obtained from a ringing choke and a simple automatic regulating system is incorporated. The arrangement is sketched in Fig. 1. The blocking oscillator V_1 develops a saw-tooth wave of about 1,000-c/s repetition frequency across C_1 and this is applied to V_2 . The anode current of this valve increases gradually during the major part of the input voltage, but when the blocking oscillator triggers for the 'fly-back' the current in V_2 is suddenly cut off. The resonant circuit formed by the anode coil with the stray capacitance is kicked into oscillation at about 25 kc/s and the peak voltage developed is around 9 kV. A voltage-tripler V_3, V_4, V_5 raises the output to 25 kV. A winding W_1 feeds a voltage proportional to the output to a diode in V_1 and the steady rectified voltage resulting across $R_1 C_2$ is applied as bias to V_2 . Thus, if the output voltage tends to increase, the extra bias on V_2 tends to offset it and so the output is maintained at a more constant level.



Direct Viewing

Development in receivers for direct viewing follows orthodox lines and the use of the line fly-back for providing the e.h.t. supply is becoming almost the standard method. The action of the circuit is substantially that of the ringing-choke system but as it also supplies the scan it can be allowed only one half-cycle of free oscil-

lation. It is usual to employ a valve rectifier with its heater run from the scan transformer and there is some step up of voltage between the amplifier and the rectifier.

In the case of a.c./d.c. sets, the h.t. voltage is limited by the mains voltage. It then becomes difficult to obtain sufficient line scan, with the result that so-called 'economy' circuits are often adopted. One such arrangement combined with the e.h.t. supply is shown in Fig. 2. V_1 is the line-scan output valve and is fed with a positive-going saw-tooth input voltage. It is cut off on fly-back and the resonant circuit formed by the transformer,

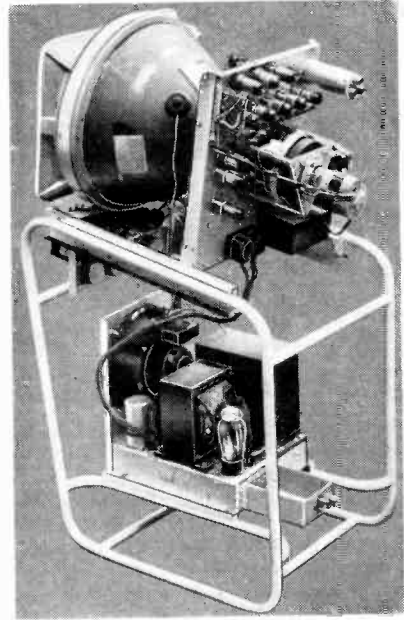


Fig. 2 (left). Typical economical line-scan circuit providing e.h.t. from the line fly-back and h.t. boost.

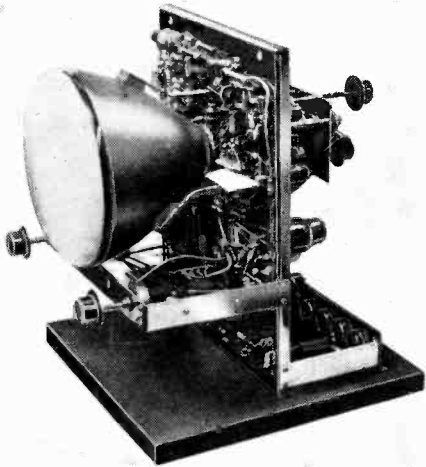
(Above). Ferranti Tr29 television chassis.

deflector coil and stray capacitance is allowed to execute about one half-cycle of free oscillation. The peak voltage on the anode of V_1 is at roughly one-quarter cycle after cut-off, and the voltage stepped up by the auto-transformer action of the primary makes V_2 conductive and charges C_4 . This capacitor acts as the reservoir and a supply of some 5-6 kV is developed

across it. The conductive period of V_2 is quite short.

When roughly one half-cycle of free oscillation has occurred the anode voltage of V_1 has fallen below the h.t. voltage to about the proper value for the start of the scan. V_3 now conducts and the energy in the magnetic field, which would otherwise cause a train of oscillations to occur, is utilized to charge C_2 through

V_3 . In doing so, the change of current in the deflector coil becomes roughly linear and is at about the right rate for the scan. The initial part of the scan, therefore, comes from the energy stored in the field at the end of the previous scan stroke. As the current decays V_1 is brought into action and provides the major part of the scan.



Chassis of Sobell television receiver.

The energy stored in C_2 , and derived from the energy in the magnetic field, is not wasted; C_2 is connected in series with the h.t. supply and the voltage across it acts to increase the h.t. supply to V_1 . With the usual mean current of 70-90 mA, the mean voltage across C_2 is of the order of 30-40 V.

With this system, control of picture width by varying the driving voltage on V_1 is hardly practicable and it is carried out by a variable inductance L_1 in series with the deflector coil. Various arrangements of the circuit are possible, but they all work in basically the same way.

On the radio-frequency side of television receivers, the trend towards the single-sideband reception of a double-sideband transmission, accepting only the sidebands remote from the sound channel, has had a rude jolt by the adoption of single-sideband transmission for the Birmingham station. As it is the sidebands adjacent to the sound channel which are retained, the avoidance of interference from the sound channel has become much more difficult. Most manufacturers have retained their normal designs for the London area and straight signal-frequency amplification with about four stages is usual.

For the Midlands area, separate models have been produced, and although some are straight sets, the superheterodyne seems to be generally preferred. Where the superheterodyne is used for both areas an interchangeable sub-chassis carrying the s.f. and frequency-changer stages is often adopted. In other cases, the whole receiver chassis may be changed.

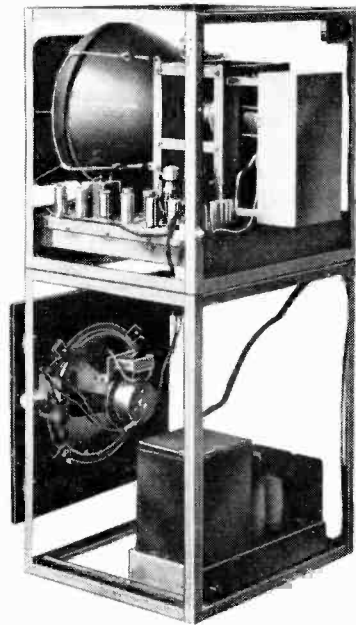
It will be interesting to see if, in the future, this principle of designing the set for the station will be adhered to, or whether the alternative of making all sets suitable for any station will be adopted. There is

certainly no sign at present that it is finding any favour.

All the small television sets have 9-in or 10-in tubes, but there are plenty with 12-in, and more firms than ever before have models with 14-in or 15-in tubes. While the small tubes operate at about 4-7 kV, the large ones are used at up to 12 kV—some 7-9 kV being usual. Several makers—notably Philco and R.G.D.—have disappearing tubes; the tube is mounted in a hinged carrier and can be pushed down right out of sight when not in use. Some other manufacturers fit sliding doors to cover the tube face.

These refinements occur only in the more expensive sets and such models often include broadcast receivers and sometimes also gramophone equipment. The small sets are usually table models or consoles for television only.

A popular television accessory is a magnifying lens. They were shown by both Acrylite and Magnavista. They are of transparent plastic, filled with oil, and give a magnification of the order of 1.2-1.5 times linear. The lens must be considerably larger than the tube face if serious distortion is not to occur and it considerably restricts the viewing angle. Because of this restriction, however, the apparent brightness of the picture is not reduced.

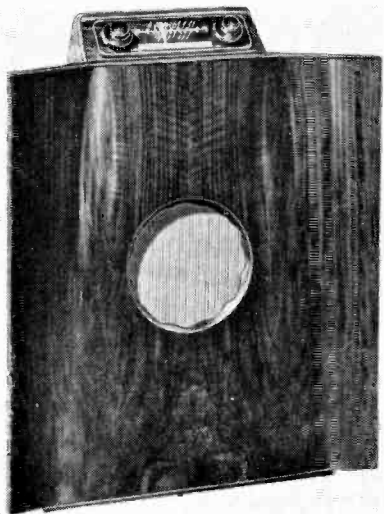


Dynatron television chassis

Broadcast Receivers

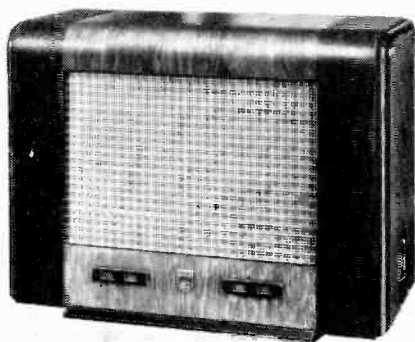
Sets for the reception of ordinary broadcast programmes show remarkable diversity of design, and range from simple 'four-valve plus rectifier' superheterodynes, shorn of non-essential complications to reduce the selling price (with tax) below the £20 level, to sets with comprehensive specifications including elaborate bandsread tuning for world-wide short-wave

listening and push-pull output stages delivering powers of the order of 10 watts for quality reproduction of home stations. Typical of this class are the Ace Radio 600, Beethoven A1188, Pye 39J/H and Philips 681A, the latter employing a double-superheterodyne circuit on short waves.



Murphy A146C baffle-type receiver.

In the search for better quality of reproduction some firms have returned to the shallow 'baffle' type of cabinet. Murphy Radio were showing several sets of this type including a console type with a frontal area of about 6 sq ft. Better diffusion of high audio frequencies is effected in some Kolster Brandes models by the use of a vertical-slot diffuser in the loudspeaker baffle. In this way the source is kept smaller in width than the wavelength up to about 7 kc/s and interference irregularities in the wave front are eliminated. Another interesting feature of K.B. sets is the use of a balancing circuit to reduce hum; h.t. line ripple of suitable phase and magnitude is injected into the tapped output transformer primary. By this means hum is economically reduced with the minimum loss of h.t. voltage.



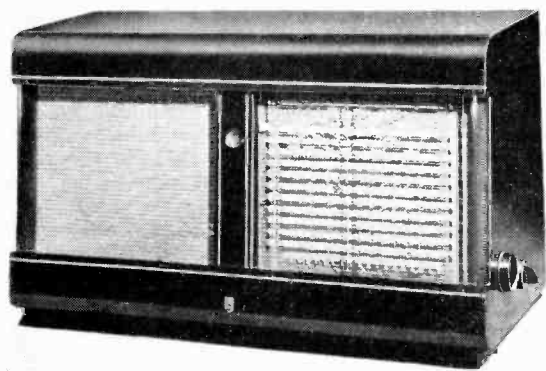
Ekco A110 'Connoisseur.'

For the greater part of the time that the average set is in use, it is safe to say that it is tuned to one or other of the local stations. To obviate the necessity for re-tuning when changing over, Ferranti Models 149 and 248 receivers have two extra positions on the wave-range switch which bring in fixed pre-tuned circuits for Home and Light programmes. E. K. Cole in their 'Connoisseur' receiver dispense altogether with continuously variable tuning and provide a switched choice of four stations—three on medium and one on long waves.

Since the last Show there has been a three-fold increase in the number of firms making portable receivers. Many are of the all-dry battery type, while a large proportion are designed to function on a.c. or d.c. mains as well as on batteries. There has also been a significant increase in the number of sets with vibrator h.t. supplies designed to operate from 6- or 12-volt car accumulators.

Car radio receivers are now being offered with short-wave ranges in addition to the usual medium and long-wave bands and push-button selected pre-tuned stations. Typical examples are the Radiomobile Type 4050 and the Ekco Model CR6r. Bandsread tuning is provided on the principal s.w. broadcast bands.

Few signs of austerity are to be found in the large radio-gramophones offered by firms such as Ace Radio, Dynatron, R.G.D., and H.M.V. The tendency is to sectionalize these large equipments so that owners can extend their scope as circumstances permit. For those who cannot find the necessary space for these luxury models, there is a wide choice of table-model radio-gramophones.



Philips 681A double superheterodyne.

Two firms, anticipating the shape of things to come, were showing production models of frequency-modulation receivers for the 90-Mc/s band. In the H.M.V. Model 1250 automatic frequency control is provided in the range 87.5 to 94.5 Mc/s while in the Kolster Brandes f.m. receiver crystal-controlled fixed frequencies are selected by a switch in the range 90-94 Mc/s.

Communications

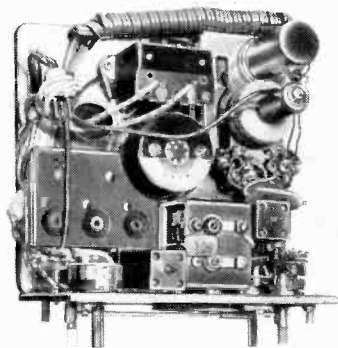
A number of new communications receivers were on view and it is interesting to find that the double-superheterodyne principle is being utilized for at least one wide-band coverage receiver, although it is not an uncommon feature in many of the v.h.f. receivers, operating

on fixed frequencies. Stratton was showing a new set of this kind, the Model 750, which covers 480 kc/s to 1,465 kc/s and 1.7 Mc/s to 32 Mc/s. The first i.f. is 1.6 Mc/s and the second 85 kc/s.

There are two features of unusual interest in the new Mullard GFR520 communications receiver. One is the exceptionally wide coverage, 540 kc/s to 110 Mc/s, and the second is the use of a special i.f. amplifier for the v.h.f. bands. From 640 kc/s to 30 Mc/s an intermediate frequency of 455 kc/s is used, but on the two highest frequency ranges, covering 27 to 110 Mc/s, it is changed to 10.7 Mc/s. The latter is a broadband amplifier of ± 50 kc/s as either f.m. or a.m. systems are catered for. The low i.f. amplifier can be varied

in bandwidth from about 10 c/s, using a crystal filter, to 25 kc/s, in six steps.

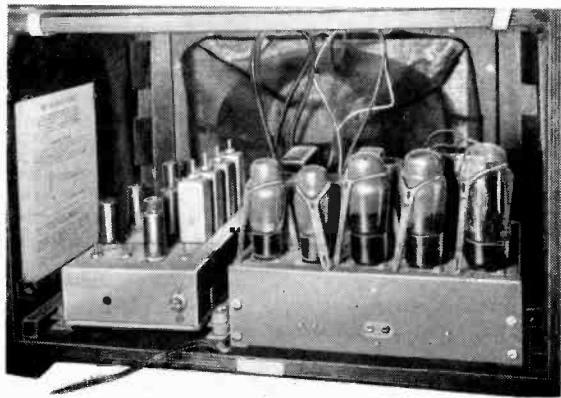
Murphy had a new version of an earlier receiver, originally a naval type, but now modified for mercantile marine use. It is described as the Model MR56,



Alfa 44 a.c./d.c. battery portable.

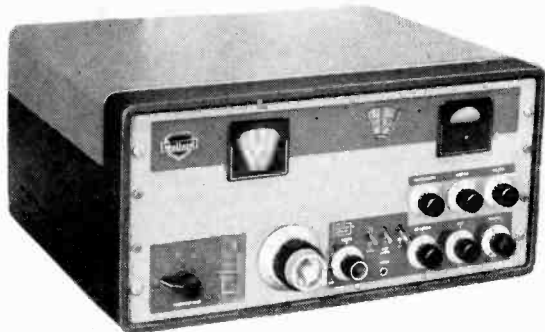
there being an A and a B version; the former covers 640 kc/s to 30 Mc/s and the latter 15 kc/s to 700 kc/s. Apart from its electrical features, one of which is the use of a self-locating coil turret, the set is notable for its very robust construction carried out in the best naval fashion.

Easy-to-operate radio-telephone equipment for use on small ships was a new feature of the communications display. One example is the Pye 'Dolphin' the transmitter of which operates on eight pre-selected spot frequencies, all crystal controlled, in the band 1.5 to 3.8 Mc/s, but the receiver covers the somewhat wider range of 530 kc/s to 3.8 Mc/s and so provides facilities for reception of broadcast programmes. It operates from either 6 or 12-V batteries.



H.M.V. 1250 frequency-modulation receiver.

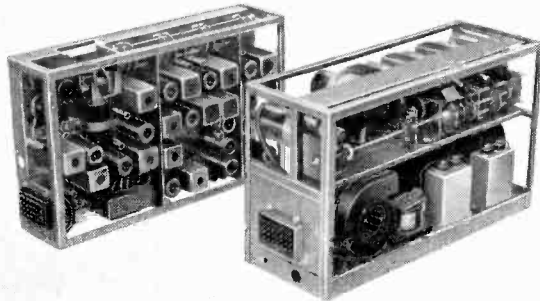
Another self-contained transmitter-receiver for trawlers and small craft is the Mullard GNE510 equipment. Its transmitter works in the 1.6 to 3.7 Mc/s band using eight spot frequencies, while the receiver gives the



Mullard GFR520 communications receiver.

choice of seven pre-set channels and one free-tuning band of limited coverage in the region of 261 metres. This set also operates on 12 volts using a rotary converter for h.t. supply.

Air and ground mobile v.h.f. equipment are developing along quite distinct lines. For aircraft use the tendency is to provide the maximum possible number of working channels in the one set with some easy channel-selecting mechanism operated from a small remote-control unit.



Murphy MR100 multi-channel v.h.f. aircraft set.

Murphy showed a set of this kind, the MR100, which provides 140 working channels in the band 118 to 132 Mc/s with 100-kc/s separation. The required send and receive channels are selected by rotary switches on a remote controller and calibrated in whole numbers and in tenths of megacycles.

Equipment of a similar kind, but covering 100 to 156 Mc/s and giving about 300 working channels of 180-kc/s spacing, was seen on Ekco's stand. The remote controller carries two lettered selector switches of 26 and 12 positions respectively and the various combinations of these give the operating channel.

Both these equipments provide crystal control of the send and receive frequencies but they do so with a limited number of crystals. The Ekco set, for example,

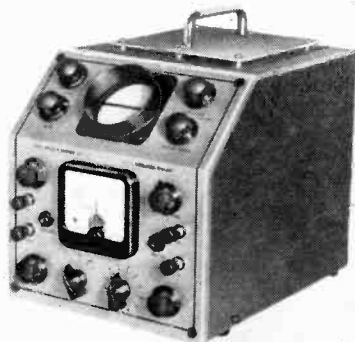
has three only and they are temperature controlled.

While most of the aircraft v.h.f. equipment is amplitude modulated, makers of the ground mobile sets offer the option of amplitude or frequency modulation. The equipment ranges in size from the small 12-lb Marconi type H19 Walkie Talkie of less than a quarter of a watt output to the 20-watt models made by the G.E.C.

A recent development in this field is the use of v.h.f. radio on trains, at least so far as this country is concerned. It apparently has to withstand very rough handling as the set shown by the G.E.C. is housed in an extremely massive iron case with heavy ribbing on the outside to assist cooling.

Test and Measuring Gear

The design of meters is now so stable that very few new types were exhibited, but it was notable that the cheapest multi-range meter in the Show (the Amplion) is obtainable with a test prod giving a 5000-V range. The most expensive (the Sangamo Weston Model S.75) provides no fewer than 53 ranges, with a sensitivity of 20,000 Ω/V on all the 14 direct-voltage ranges, and self-contained measurement up to 500 M Ω at 500 V. Few even of the valve-assisted meters can better this, but a notable exception is the Burndept high-resistance test set with a top reading of 10¹⁴ Ω . This is achieved by using a pair of electrometer valves in push-pull which are coupled to a pair of triodes with the indicating meter connected between their cathodes.

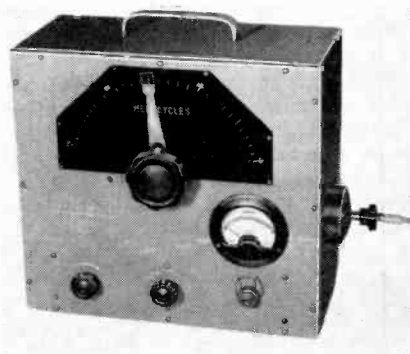


*E.M.I. Q/D. 101
oscilloscope.*

A new oscilloscope, the E.M.I. No. Q/D.101, is a compact model intended mainly for servicing purposes, but useful also as a laboratory instrument on account of its built-in valve voltmeter with ranges from 0-5 V to 0-500 V, positive or negative. It has been arranged to read the peak voltage relative to a horizontal line across the c.r. tube face, so that by using the vertical shift the voltage of any part of a waveform can be measured directly.

The tendency with audio sources is towards more extended frequency ranges. The new B.S.R. Type LO 400/100, for example, covers 10-100,000 c/s, and follows the usual practice of this maker in being of the beat-frequency type, with two dials and no range-switching. The fine-reading dial, scaled 10-2,500 c/s, controls the 'fixed' oscillator, and its reading is to be subtracted from that of the main dial at any setting of the latter. An addition to the Advance signal generators is the Model H-1, covering 15-50,000 c/s in three resistance-capacitance ranges. Two valuable features, unusual in such a moderately-priced instrument, are continuously-variable output from 200 μV to 20 V,

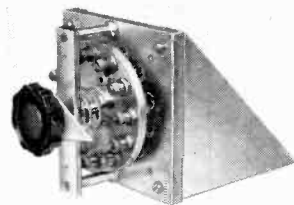
accurate to ± 1 db, and alternative sine and square waveforms. Harmonics of the latter are detectable up to about 20 Mc/s. The E.M.I. a.f. test set, Q/D.041, is also of the RC type, but is considerably more than



Pye television signal generator.

an audio source. It incorporates a valve voltmeter and amplifier which enable it to be used for a wide variety of tests and as both source and detector for bridges. The same firm showed two bridges suitable for use in conjunction with it—one covering wide ranges of L, C and R, and the other a distortion bridge in which the fundamental in the output from the amplifier under test can be balanced out, leaving the harmonics measurable.

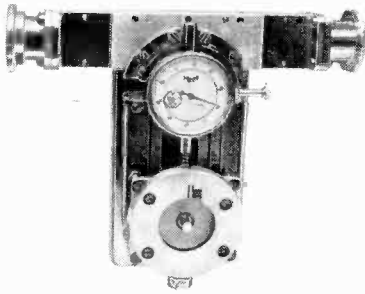
R.F. signal generators, such as the AVO model, which formerly just took in the London television frequency, have had the frequency ranges extended to cover all the television channels. And several new models designed primarily for television appeared, such as the Pye and the Taylor. The former is provided with 400-c/s 30% sinusoidal modulation for testing the sound channel, and 400-c/s and 60-kc/s 100% square-wave modulation for setting up a grid pattern on the vision screen; the output is controlled by a calibrated piston attenuator. Factory equipment for the television manufacturer was exhibited by Burndept, comprising a central rack connected by coaxial cable to the test bays. The rack equipment is arranged to contain the required number of signal-generator units, each providing an alignment frequency within the band 52-100 Mc/s, and consisting of an oscillator stage, a modulatable power amplifier,



*Burndept co-axial
switch unit.*

and a cathode-follower output stage. The unit at each test bay contains a 12-way co-axial switch for selecting any of the signals from the central rack, while preserving the correct termination and full screening for all the lines, and also an attenuator and signal-level indicator employing a CS₂C crystal rectifier. The maximum frequency drift in an 8-hour day is stated to be + 50 kc/s at 50 Mc/s. An important new instrument is the TS71 30-100 Mc/s

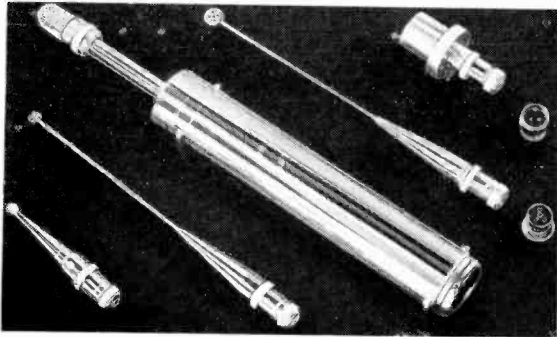
portable interference-tracing set, made by Murphy for the G.P.O. Though primarily intended for the investigation of complaints of interference with the television programmes, it has been designed to cover also f.m. broadcasting and official and business v.h.f. communications. The set consists of a battery-driven superheterodyne using a multi-grid mixer and separate oscillator to yield a 3-Mc/s intermediate frequency. This is amplified in four stages with a 100-kc/s bandwidth and fed to two separate diode-pentode valves, one for a meter indicator and the other for listening. To avoid the critical tuning inseparable from a b.f. oscillator, unmodulated carriers are made audible by causing the second i.f. valve to modulate the signal. The total weight, including two aeriels, headphones, and batteries, is only 22 lb.



For field-strength measurements in this band, two new sets were shown. The Murphy FSM22 uses first-stage noise as the reference level, and like the TS71 has

Metrovich attenuator Type 82.

been designed to meet G.P.O. requirements. To cope with impulsive noise, the circuits have been designed to be linear up to no less than 100 times full-scale deflection, and to this end the last i.f. stage is in push-pull. The time constants of the detector are to C.C.I.F. standards. The Marconi Instruments TF930, on the other hand, incorporates a standard signal generator for calibration. The range covered is 18-125 Mc/s, and the dipole aerial is adjustable to 0.42λ at any frequency in this range.



Cosmocord wide-range probe microphones.

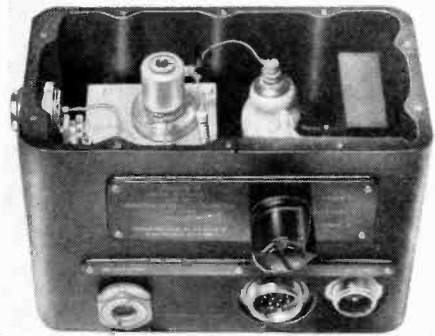
Examples of instruments for accurate measurements in the 3-cm band were shown by Metropolitan-Vickers, for Ministry of Supply research. These indicated a considerable advance in precision over the waveguide apparatus of a few years ago. In the standing-wave detector, variations in probe penetration as it is moved

along are kept within ± 0.0001 in. The attenuator is provided with a glass vane with an evaporated coating of nichrome covered by a protective fluoride layer. The maximum attenuation is 40 db, with a resetting accuracy of 0.5 db and an absolute accuracy of ± 0.5 db. In a cathode-ray standing-wave detector, the standing waves set up in any section of waveguide connected to it are shown graphically on the screen.

Among the miscellaneous items of equipment may be mentioned a unit by E.M.I. for dealing with that bugbear of the service depot—the intermittent fault. Described as the automatic monitor Q/D 231, it provides three channels, to deal with up to three suspected receivers simultaneously. A 1000-c/s multivibrator generates a signal spectrum over the whole r.f. range up to 10 Mc/s. This is applied to the input of a receiver under test, and the output is fed into the monitor, which gives audible and/or visual warning of any variation in output level.

Airmec showed a material comparator having a wide range of usefulness, as samples of material can be compared for size, conductivity, permeability, etc., by inserting them into a suitable jig overwound by a coil forming one arm of a bridge. A similar arm, balanced against it, contains a standard sample. Lack of balance is shown in magnitude and phase on a c.r. tube.

To correspond with the growing use of high voltages, the ionization insulation tester by the same firm is now available with test voltage variable up to 25 kV.



Ekco vibrating-reed electrometer.

Lastly, a new range of acoustical instruments was shown by Cosmocord, making use of the stabler piezoelectric materials, lithium sulphate and ammonium dihydrogen phosphate. Among these was a standard artificial ear, and a sound-pressure standard consisting of a cylindrical pre-amplifier (2 stages and cathode-follower) with alternative crystal microphones attached. The latter was designed primarily for under-water sound-pressure measurements, for which (owing to the relatively long wavelength in water) its frequency range is 100 kc/s to 100 kc/s; but it is equally suitable for measurements in air up to 20 kc/s. Blast pressures up to 10^7 dynes/cm² can be measured.

Most of the equipment in the industrial and medical fields showed little development since this year's Physical Society exhibition; but a logical tendency to provide hearing aids with radio reception was noticeable. The Aurotone models include within the normal hearing-aid

dimensions no less than a 4-valve superheterodyne. A simple one-station pre-set circuit is available in aids by John Bell and Croyden, which are interesting as examples of circuit printing, using the colloidal-silver process.



Microgroove recorder used in radiogramophones by M.S.S.

Equipment for detecting and measuring the various kinds of radioactivity was shown by Airmec, Dynatron, Ekco, G.E.C., and Marconi Instruments. A special division of E. K. Cole, in close co-operation with the Atomic Energy Research Establishment, has developed a wide range of apparatus suitable for large and small scale work in this field. Items shown included a range of portable radioactivity monitors using ionization chambers with 'windows' appropriate to the type of radiation to be measured; a linear amplifier; a super-stabilized low-noise power unit; an impulse counter; a ratemeter; a c.r.t. monitor; and a typical rack-mounted assembly—a Geiger-Muller unit, counter, monitor and power supplies.

In the power unit, of the rectified r.f. type, unusual precautions proved to be necessary to reduce noise to the low level concomitant with its high degree of stability and low ripple. The output of 1 mA is continuously variable between 250 and 3,000 V positive or negative, with a stability of 0.05% against 10% mains variations. Ripple, noise and pulse content at 3,000 V is not more than 250 μ V.

In the Ekco vibration electrometer, the extremely small unidirectional currents to be measured are adapted for a.c. amplification by applying them in series with a resistance of $10^9 \Omega$ to a fixed gold-plated anvil forming, with a vibrating reed, a capacitance varying at audio frequency. To exclude leakage across the input resistor, whose resistance may be as high as $10^{12} \Omega$, the input and vibrator portion, with the first stage of the amplifier, are enclosed in a hermetically-sealed head.

Sound Reproduction

In pickup design the most noteworthy advances are in styli. Satisfactory methods have been evolved for the production of diamond points, which are now available as an alternative to sapphire or tungsten carbide in the Decca and Lowther pickups. Several firms are offering interchangeable heads with points for

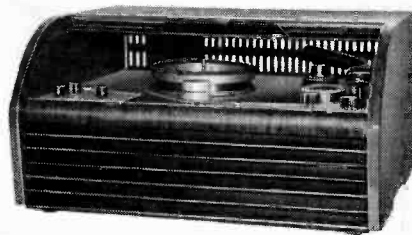
standard or 'microgroove' long-playing records. In the Goldring 'Headmaster' pickup one of the heads has a large-radius point (0.0035 in) for use with old or noisy records, and is said to give an improved signal/noise ratio.

Among loudspeakers one of the most interesting exhibits was a high-quality reproducer by the Acoustical Manufacturing Co. with a ribbon-diaphragm h.f. unit, and l.f. cone unit loaded by a two-stage acoustic filter. A double-cone unit with independent voice coils working in separate air gaps in series was shown by Whiteley Electrical Radio. Many of the permanent-magnet loudspeakers have now reached flux densities of 17,500 gauss in the gap, and 19,500 gauss is the figure given for the Lowther-Voigt p.m. unit.

There is evidence of increased interest in sound recording and six firms were showing disc-recording equipment. A moving-coil cutter head is used in the new machine designed by A. R. Sugden, and M.S.S. included a microgroove recorder in a comprehensive exhibit of portable and studio machines. Magnetic iron-oxide coated tape recorders were shown by G.E.C., R.G.D. and Wright and Weaire, and wire recorders by Kolster Brandes and Simon Sound Service.

Accessories

Among developments of unusual interest to battery users was a new type of accumulator shown by Exide. It has a moulded polystyrene case and lid and a new-type of absorbent plate separator. This separator is made of Lignex which is described as being so absorbent that it holds in suspension all the acid the cell needs. Thus by including a lid with quite a shallow acid trap the cell is easily made unspillable without a noticeable increase in overall dimensions. When the cell is inverted only a minute amount of free acid falls into the acid trap. This cell is known as the Exide JSP2 and is of 14-AH capacity.



Kolster-Brandes EWR60 wire recorder.

Another development is the Kalium cell shown by Burndept and Vidor. It is claimed to have from four to seven times the watt-hour capacity of an equivalent size of Leclanché cell, to show no appreciable drop in voltage through its life and not deteriorate in store even at relatively high temperatures.

There are five sizes available which in physical dimensions are equivalent to the B.S.S. U1 to U7 (U3 and U5 are not included) the Vidor-Kalium equivalents being Vor01 to Vor07. So far its application is limited to l.t. supplies but it has distinct possibilities in other fields.

In its constructional form it is similar to the Leclanché type for it has a central carbon rod, which is the positive pole, and a zinc case forming the negative. The electrolyte is mainly caustic potash and the depolarizer mercuric oxide mixed with powdered carbon. The cell has a low internal resistance which is maintained right up to the end of its useful life.

Power supply in another form was the main feature of the Westinghouse exhibit and this year they had a new e.h.t. unit for television receivers which provides 6kV from the flyback pulses across the line output transformer. It is a voltage tripler having three type 36EHT35 rectifiers and five capacitors and its overall size is $2\frac{3}{4}$ in square by $3\frac{1}{2}$ in high.

One of the most interesting of the new valves was the Osram A1824 disc-seal tetrode. The electrodes are not arranged in the co-planar form usual for disc-seal triodes, but are assembled as concentric cylinders. The contact rings are arranged to allow the valve to be embodied in a concentric-line circuit, for it is capable of giving a useful output up to 500 Mc/s. At 400 Mc/s the output is 150 W and at 100 Mc/s it is 185 W. The copper anode is heavily ribbed, and forced-air cooling is used.

Also in the Osram range is a new double tetrode, the TT17, for use up to 250 Mc/s. It is designed for 19-V operation and is apparently intended primarily for aircraft equipment. The anode dissipation is 40 W total and there is a built-in by-pass capacitor between the screen grids and cathode.

Brimar showed a new transmitting tetrode in the form of the type 5703 for use up to 150 Mc/s. The anode dissipation is 12 W and an interesting feature of its construction is that two separate input grid leads are

provided. They join to separate pins on the B9A base and it is claimed that the dual input assists grid cooling and also gives a lower input impedance than would otherwise be obtainable. It is a 6-V valve taking 0.75 A heater current.

Components

It now seems certain that the miniature component has come to stay and that it can no longer be regarded as a novelty. There is, of course, no reason for making a component larger than is necessary for efficient operation. In some cases, however, miniaturization calls for very great precision in manufacture, a case in point being the latest range of Polar miniature variable capacitors. A nominal 0.0005- μ F two-gang capacitor measures only $1\frac{1}{2} \times 1\frac{1}{2} \times 2\frac{1}{4}$ in. Some idea of the precision work involved in its assembly can be gauged from the fact that the vane spacing is only 0.009 in.

Fixed capacitors all follow the same general trend and Hunt have developed a new process for the construction of miniature metallized paper capacitors up to 0.01 μ F in value. The finished article, measured over a cylindrical moulded case of hard resinous compound, is $\frac{3}{8}$ in long $\times \frac{1}{8}$ in diameter.

An exceptionally versatile form of potentiometer has been evolved by Eric. Known as a stud potentiometer it takes the form of a stud switch on which can be assembled up to nine miniature fixed resistors. Any combination of resistors can be used and changed, if necessary, at any time. With the back cover on, it looks like any ordinary volume control, even to the inclusion of a mains switch but the inclusion of the switch necessitates omitting two of the potentiometer studs, thus reducing the usable resistance steps to seven.

CORRESPONDENCE

Letters to the Editor on technical subjects are always welcome. In publishing such communications the Editors do not necessarily endorse any technical or general statements which they may contain.

Interelectrode Capacitance of Valves

SIR,—I am indebted to Mr. R. H. Booth¹ for drawing attention to two papers which had escaped my notice. I was particularly interested in his remark on the effect of the variation of field along the surface of the cathode, due to the shielding effect of the grid wires. The importance of this factor had occurred to me and I am in full agreement that this explains the gradual rise in grid-cathode capacitance. Measurements carried out for clarification gave the following values of μ in triode 6J5,

$$V_a = 100 \text{ V, } i_a = 5 \text{ mA, } \mu = 25,$$

$$V_a = 100 \text{ V, } i_a = 0.2 \text{ mA, } \mu = 20,$$

$V_a = -200 \text{ V, } V_g = +4 \text{ V, } i_g = 0.12 \text{ mA, } \mu = 62,$ showing a variation in μ of more than 1:3 along the surface of the cathode.

The curves on the grid-cathode capacitance in a recent paper² seem to me revealing in this connection. In the valves DET 22 E and DET 22 F which, out of a series of otherwise identical valves, have the largest distance from grid to cathode, the grid-cathode capacitance rises sharply as soon as emission starts. The sharp rise indicates that emission starts almost simultaneously along the whole of the cathode, which is to

be expected, as in this case the field along the cathode is the most uniform.

North, in his paper, disregards the lack of homogeneity along the cathode and, for this reason, his formula cannot be expected to show the effects caused by differences in construction. For instance, in the paper by Humphreys and James, Fig. 8, p. 29, the part of C_{gk} which in North's formula is independent of g_m seems to be anything between 10 per cent and 50 per cent, instead of the required 33 per cent.

The value of 10 per cent occurs in the valve having a very small distance from grid to cathode. The shielding effect of the grid wires is particularly strong and emission may be assumed to take place mainly between the wires of the grid. In the path of the electrons the field perpendicular to the cathode rises considerably from cathode to grid, whereas North discusses the case of a constant field. The transit time from cathode to grid is hence smaller than is assumed in the theoretical derivation and, therefore, the electron density is smaller as well. Naturally, in assessing the curves one must not forget that the cold capacitance from grid to cathode is also smaller than the theoretically assumed value.

An increase of capacitance larger than the theoretical

value occurs in the valve having a fairly large distance from cathode to grid. Above it was assumed from the capacitance curve of this valve that the whole of the cathode starts emitting simultaneously. It seems probable that the large increase in capacitance is caused by electrons coming from parts of the cathode shaded by the grid wires. On approaching the grid they pass through a decreasing field and are deflected from their straight path towards the plane halfway between the wires. Their density will be disproportionately large and so will be their contribution to the grid-cathode capacitance.

As to the increase in capacitance 'beyond cut-off,' we have recently measured the capacitance between suppressor grid and cathode of an r.f. pentode. The cold capacitance is naturally extremely small, but there is a slight increase when emission starts even when suppressor-grid and anode voltage are at -40 volts. Any current flowing to the suppressor grid seems out of the question and the effect appears of the same nature as that observed beyond cut-off. If we try to explain our observations, according to van der Ziel's theory, on continued emission it is difficult to account for the complete disappearance of any increase in grid-anode capacitance.

E. E. ZEPLER.

University College, Southampton.

REFERENCES

- ¹ *Wireless Engineer*, June 1949, p. 211.
- ² B. L. Humphreys and E. G. James "Interelectrode Capacitance of Valves" *Wireless Engineer*, January 1949, p. 26.

Valve Noise and Electron Transit Time

SIR,—I have just noticed that in your April issue* Mr. D. B. Fraser quotes me as suggesting that 'the noise in thermionic valves arises from variations in the emission velocities of the electrons,' and proceeds to point out that emission velocity is of negligible significance in temperature-limited operation.

Never in any paper have I suggested that emission velocity was relevant to the magnitude of noise from a temperature-limited diode, and I do not see how this misunderstanding can have arisen. I have, however, pointed out that as between the temperature-limited diode on the one hand and the metallic conductor on the other, there is an *exchange of role* between the steady drift velocity due to the applied field and the random thermal velocities, as follows.

In the temperature-limited diode the transit time is for practical purposes fixed by the externally-applied anode voltage and so, therefore, is the noise spectrum. (It turns out to be independent of the applied voltage except at frequencies high enough to introduce the factors studied by Mr. Fraser). But in the metallic conductor, the effective 'transit time' is the time of free flight of an electron between collisions with the lattice, and this is governed by the thermal-agitation velocities which are much larger than the drift velocity which can be produced by any practicable potential gradient.

I trust that this will clear up the question of temperature-limited diodes. I do not wish to embark on a new controversy on the validity of the idea of a 'frequency spectrum,' which I have used above because it is intelligible to most engineers. So if any readers object to 'noise spectrum,' will they please substitute 'the form of the time-function which describes the varying part of the current.'

D. A. BELL.

The University,
Birmingham.

* "Noise Spectrum of Temperature-Limited Diodes" *Wireless Engineer*, April 1949, Vol. 26, p. 120.

Transit-time Effects in U.H.F. Valves

SIR,—In his recent paper¹ Dr. Thomson derives the well known^{2,3} expression for the parallel resistance of an electron beam between parallel electrodes at the same direct potential with an impressed a.c. field. The expression is:

$$R_p = \frac{2V_0}{I} \cdot \frac{I}{F(\theta)} \dots \dots \dots (A)$$

$$\text{with } F(\theta) = \frac{2(1 - \cos \theta) - \theta \sin \theta}{\theta^2} \dots \dots \dots (B)$$

In discussing this result Dr. Thomson says that it is identical, with the exception of a multiplying constant, with Llewellyn's analysis⁴ of a plane parallel space-charge limited diode, and concludes that since the dependence on transit angle is the same, the Llewellyn result must be regarded with suspicion. In fact, however, Llewellyn's result for a diode is quite different as is immediately obvious from a comparison of Thomson's Fig. 5 with Llewellyn's Fig. 2. For a series impedance representation Llewellyn's result in Thomson's notation is:

$$R_s = \frac{12R_0}{\theta^2} \cdot F(\theta) \dots \dots \dots (C)$$

where R_0 = static slope of the diode. The physical validity of (C) can be seen as the low-frequency value $\theta \rightarrow 0$, is R_0 while (A) leads to an infinite parallel resistance as $\theta \rightarrow 0$; i.e., to zero series resistance. Since the analysis of the space charge limited diode does not lead to the same result as that of a v.m. tube grid there is no reason to doubt the general correctness of the Llewellyn analysis.

Dr. Thomson has already⁵ corrected the derivation of his equation (16) for the damping of a diode in the retarding field-region.

$$\text{This is given by } R = \frac{V_0^2}{8V_g} \cdot \frac{I}{I} \cdot \frac{I}{F(\theta)} \dots \dots \dots (D)$$

where V_g = retarding voltage.
 V_0 = voltage corresponding to the initial velocity.
 I = saturation emission.

Equation (D) can be rewritten in a rather simple form as follows: the electrons have a Maxwellian velocity distribution so we can use the mean-square velocity to obtain V_0 ; i.e., $V_0 = kT/e$.

Furthermore, in the retarding field region $I_a = I \exp(-eV_g/kT)$ where I_a = current reaching the anode.

Inserting these expressions we obtain:

$$R = \frac{1.08T + 10^{-5} (\log_e I_a - \log_e I)^2}{I} \cdot \frac{I}{F(\theta)} \dots \dots \dots (E)$$

Equation (E) could be checked rather easily by measuring R as a function of I_a in the region $0.8\pi < \theta < 1.3\pi$ where $F(\theta)$ is constant to within about 10 per cent. Equation (E) is naturally only valid for values of I_a small enough to ensure that the valve is really operating in the retarding field region.

Standard Telephones & Cables, Ltd. A. H. BECK.
Enfield, Middx.

REFERENCES

- ¹ *Wireless Engineer*, June 1949, p. 192.
- ² "Klystrons & Microwave Triodes," Hamilton, Kuper & Knipp, McGraw Hill, 1948.
- ³ "Velocity Modulated Thermionic Tubes," Beck, Cambridge University Press, 1948.
- ⁴ "Electron Inertia Effects," Llewellyn, Cambridge University Press, 1941.
- ⁵ *Wireless Engineer*, August 1949, p. 278.

SIR,—Mr. Beck's equation (C) is correct, and my equation (11) which should have read $R_2 = R_0 I'(\theta)$,

where $R_{\theta} = 12R_0/\theta^2$ is wrong. In condensing the argument for publication, I wrongly interpreted equation (11). I can only regret the error. Nevertheless, the contention that Llewellyn's result is suspect arises from a study of his development of this equation for, as suggested in paragraph 5 of my paper, Child's law demands the approximation that the electric field at the cathode is zero, and Llewellyn's 'complete space-charge' is defined as the state where 'the emission of zero-velocity electrons from the α -plane (virtual cathode) is sufficient to reduce the electric field at that plane to zero.' My doubt arises from the fact that the potential minimum, itself due to the distribution of velocities of emission, is not at the cathode, for while this is unimportant in many cases, it is a serious factor in determining the transit angle.

In the second paragraph of his letter Mr. Beck derives an interesting expression for the diode damping in the retarding field. Since the derivation here is wholly in terms of potential energy, it appears to be independent of the existence of a space charge, but in the region where V_G and V_0 are of the same order of magnitude the equation will no longer be true.

Royal Naval College,
Greenwich.

J. THOMSON.

Negative-Feedback Amplifiers

SIR,—In his letter in your September issue, Mr. McLeod gives an able summary of Bode's work on the above subject. The cut-off slope of 12 db/octave is, of course, the theoretical limit: some reduction is necessary to afford a phase margin and Bode prefers 10 db/octave.

I cannot agree that the 'natural' frequency characteristic of a three-stage amplifier 'requires only slight modification . . . just outside the pass-band . . . ' to change it into Bode's ideal characteristic, which has a sharp corner at the edge of the band and an attenuation of 19 db in the first subsequent octave. Quite a number of inductors and capacitors are required to obtain a reasonable approximation to this shape.

I think Mr. McLeod is mistaken in stating that the maximally-flat amplifier requires a frequency characteristic (this must surely be the design point Mr. McLeod had in mind) controlled up to higher frequencies than the Bode design. Bode's frequency characteristic has a specified shape up to a frequency about an octave higher than that at which the loop amplification becomes unity: the maximally-flat amplifier cuts off on the natural asymptote provided by the stray capacitances. Mr. McLeod mentions the effect of stray inductances: 25 pF resonates at 100 Mc/s with 0.1 μ H, where the reactance is 63 Ω . The effective stray inductance in an ordinary well-designed intervalve coupling is not likely to reach 0.05 μ H if the circuit contains only the essential basic components, but if there is a complicated network to control the cut-off characteristic, larger stray inductances may occur. Mr. McLeod's difficulty with them may, therefore, be due to the inclusion of the equalizers necessitated by the Bode method.

Apart from these points of detail, Mr. McLeod and I now appear to be in agreement.

Redburn, Herts.

C. F. BROCKELSBY.

Constant Phase-shift Networks

SIR,—I wish to comment on Mr. R. O. Rowlands' article in the September 1949 issue of *Wireless Engineer*. He introduces a design method for constant phase-shift networks in which the performance and design of such networks is related to those of allied attenuation net-

works. The essential feature of his ingenious method is to transform a performance characteristic with upper and lower limits into one with one kind of limit only, thus simplifying the design procedure considerably. I should like to point out that this can be achieved—by using Mr. Rowlands' own method—without introducing the concept of an allied attenuation network, thus further simplifying the theory and design procedure. For this purpose, starting with Mr. Rowlands' equation (5) and retracing some of the steps in his derivation

$$\text{we find } j\beta = \log_e \frac{x+jy}{x-jy} = 2j \tan^{-1} \frac{y}{x}$$

$$\text{and therefore } \log_e \left| \cot \left(\frac{\beta}{2} - \frac{\pi}{4} \right) \right| = \log_e \left| \frac{x+y}{x-y} \right|$$

Since in the ideal case $\beta/2 = \pi/4$, there is now a lower

limit only, viz., for $\log_e \left| \frac{x+y}{x-y} \right|$. This expression can be

expanded in the form $\sum_{\lambda=1}^{\infty} \log_e \left| \frac{1+h_{\lambda}\omega}{1-h_{\lambda}\omega} \right|$. Now $\log_e \left| \frac{1+h\omega}{1-h\omega} \right|$

$= 2 \tanh^{-1} h\omega$ or $2 \tanh^{-1} \left(\frac{1}{h\omega} \right)$, depending on whether

$\omega > h\omega$ or $\omega < h\omega$. Thus we are led directly, without the introduction of an attenuation network, to the graphical method described by Mr. Rowlands. If this derivation is adopted, the db-scales in Figs. 3 and 4 can be replaced by corresponding degree scales (deviation from 90°), in accordance with the relation given in Fig. 2.

However, a db-scale with physical significance could be introduced by considering the use of two phase-shift networks with phase-shift difference β for a single-sideband modulator. Then the response curves for the wanted and the unwanted sideband are given by $\alpha_1 = 10 \log_{10} (1 + \tan^2 \delta/2)$ and $\alpha_2 = 10 \log_{10} (1 + \cot^2 \delta/2)$, respectively, where $\delta = \beta - \pi/2$. If Mr. Rowlands' db-scale is designated by α_0 , the relation between α_0 , α_1 and α_2 is given by $10\alpha_1/10 = 1 + 10^{-\alpha_0/10}$ and $10\alpha_2/10 = 1 + 10^{+\alpha_0/10}$.

In Figs. 3 and 4, Mr. Rowlands uses for representing the expression $\log_e \frac{1+h\omega}{1-h\omega}$ a pair of straight lines in a co-

ordinate system with a functional scale for the ordinate axis, rather than a non-linear curve in conjunction with a linear scale. It may be of interest to note that I and my associates have for a number of years used this principle of straight-line graphs in filter design, usually in a modified form where the pair of straight lines is replaced by a single straight line and the ordinate axis duplicated. A publication dealing with various straight-line graphical methods is in preparation.

I have recently investigated the problem of designing constant phase-shift networks by purely analytic—as opposed to graphical methods. Explicit design formulae for networks for any bandwidth and any degree of approximation to the nominally constant phase-shift value (for Tchebycheff as well as Taylor approximations) have been found. A detailed account will be published.

W. SARAGA

Telephone Manufacturing Co., Ltd.,
St. Mary Cray, Kent.

GAIN OF AERIAL SYSTEMS

Reference 16 was omitted from this article in the September issue (p. 306). It should be to "The Theoretical Precision with which an Arbitrary Radiation Pattern may be obtained from a Source of Finite Size," by P. M. Woodward and J. D. Lawson, *J. Instn. elect. Engrs*, Part III, September 1948, Vol. 95, p. 363.

WIRELESS PATENTS

A Summary of Recently Accepted Specifications

The following abstracts are prepared, with the permission of the Controller of H.M. Stationery Office, from Specifications obtainable at the Patent Office, 25, Southampton Buildings, London, W.C.2, price 2/- each.

ACOUSTICS AND AUDIO-FREQUENCY CIRCUITS AND APPARATUS

623 205.—A wide-band loudspeaker with light-weight coil and diaphragm vibrating independently, the centering and current feed to the coil being at a point remote from the connection to the diaphragm.

Standard Telephones and Cables Limited (assignees of Le Matériel Téléphonique). Convention date (France) 7th June, 1943.

AERIALS AND AERIAL SYSTEMS

623 770.—A waveguide for a common T/R aerial system in which a receiving probe is designed for E-mode waves and a transmitting probe for H_{11} waves; a dielectric block transforming the polarization of the transmitted wave so as to have no effect on the nearby receiving probe.

E. Coop. Application date November 21st, 1946.

624 091.—An u.s.w. cavity-resonator aerial of the directive type having a long and narrow slot in a quadrangular box which contains a conductor transversely behind the slot.

Radio Corporation of America. Convention date (U.S.A.) August 25th, 1945.

624 876.—Directive aerial array designed for reducing the side lobe, and having an auxiliary array to reduce side-lobe amplitude of a main array.

Western Electric Company Incorporated. Convention date (U.S.A.) December 15th, 1944.

DIRECTIONAL AND NAVIGATIONAL SYSTEMS

623 635.—D/F equipment in which sense ambiguity is avoided, wherein alternate minima are selected by a rectifier which provides a positive or negative output according to the phase of the carrier wave.

C. G. Kemp. Application date October 18th, 1945.

624 725.—Change of a radio frequency by the Doppler effect is used to ascertain rate of approach of an object; the operative frequencies are converted into intermediate frequencies from which low-frequency beats are obtained.

Sperry Gyroscope Co. Inc. Convention date (U.S.A.) November 21st, 1945.

RECEIVING CIRCUITS AND APPARATUS

(See also under Television)

621 267.—Bandspread system in which a suitably designed tuning capacitor is mechanically coupled to a variable reactance element to give a uniform scale for the medium and long bands.

Philips Lamps Limited. Convention date (Netherlands) 11th March, 1944.

621 803.—F.M. receiver using spaced aerials with phase and amplitude adjusters to reduce beat interference.

Standard Telephones and Cables Limited (Assignees of G. T. Royden). Convention date (U.S.A.) 21st July, 1945.

621 993.—Heterodyne circuits for u.h.f. in which the signal is fed to the mixer through a resonator having a core and a cylindrical sheath.

Westinghouse Electric International Co. Convention date (U.S.A.) 22nd September, 1943.

622 099.—Limiter for f.m. receivers using a valve with a control grid operating by anode-current saturation.

The British Thomson-Houston Co. Ltd. Convention date (U.S.A.) 12th April, 1944.

622 479.—Motor-operated a.f.c. systems using a control valve forming part of a bridge network to operate motor-control relays.

Marconi's W.T. Co. Ltd. and G. L. Gridale. Application date 2nd July, 1946.

623 581.—Permeability tuner in which parallel iron cores on a common carrier are moved relatively to tuning coils by a cam.

Weymouth Radio Manufacturing Co. Ltd., and B. I. Jordan. Application date November 12th, 1946.

624 007.—Discriminator circuit for f.m. and like systems wherein loading of the primary circuit of a Seeley discriminator by the rectifier is reduced by the introduction of negative resistance into the primary circuit.

Radio Corporation of America (assignees of W. R. Koch). Convention date (U.S.A.) August 3rd, 1945.

624 010.—A common potentiometer is used both for r.f. volume control and for controlling negative feedback in the a.f. part of a receiver.

Philips Lamps Ltd. Convention date (Netherlands) March 5th, 1943.

624 535.—A receiver and cabinet, in which the chassis rests on backwardly-sloping runners and the tuning panel is positioned against an inclined window in the cabinet.

Kolster Brandes Ltd., P. H. Spagnoletti and D. A. J. Bassam. Application date April 29th, 1947.

TELEVISION CIRCUITS AND APPARATUS

FOR TELEVISION AND RECEPTION

621 479.—Sound is transmitted on a television carrier by means of modulated pulses timed within the synchronizing pulses.

D. I. Lawson, A. V. Lord and Pye Ltd. Application date 12th October, 1945.

621 560.—Colour television wherein a black image is transmitted over a common channel as well as images for the three primary colours.

Marconi's W.T. Co. Ltd. (Assignees of A. N. Goldsmith) Convention date (U.S.A.) 21st August, 1942.

622 202.—Colour television using a rotary colour filter wheel synchronized by received signals.

Marconi's W.T. Co. Ltd. (Assignees of F. J. Somers) Convention date (U.S.A.) 19th October, 1944.

622 656.—Choice of shunt feed inductance for c.r. deflection circuits wherein deflection coils are fed through a capacitor.

Philips Lamps Ltd. Convention date (Netherlands) 20th March, 1942.

624 022.—Constant amplitude time base of variable frequency, the attainment of predetermined potentials affecting the change from sweep to fly-back and vice versa.

Cinema-Television Ltd. and J. M. Sowerby. Application date 16th December, 1946.

624 417.—Interlaced film-scanning apparatus with continuous film movement, using a scanning disc with two sets of spiral-path apertures and independent optical systems in each path to compensate for different speeds of the two sets of apertures.

The General Electric Co. Ltd., and D. C. Espley. Application date October 17th, 1945.

624 832.—Cathode-ray tube circuit in which the cathode is heated by cyclically varied bombardment, e.g. during the flyback, to avoid delocating due to secondary electrons.

Cinema-Television Ltd. and W. H. Buchanan. Application date July 10th, 1947.

TRANSMITTING CIRCUITS AND APPARATUS (See also under Television)

620 680.—Velocity-modulated oscillator is switched off and on for duplex working by controlling the loading of the tank circuit.

Marconi's W.T. Co. Ltd. (assignees of O. E. Dow). Convention date (U.S.A.) 10th June, 1942.

620 828.—Valve keying of a transmitter power amplifier by means of a controlling pentode connected between the amplifier cathode and earth.

Standard Telephones & Cables Ltd. (assignees of Le Materiel Telephonique Société Anonyme). Convention date (France) 11th April, 1945.

621 386.—Frequency control of magnetrons and like sources is effected by a control impedance which is transformed to an impedance having a higher Q . The problems of frequency stabilization are examined mathematically.

Marconi's W.T. Co. Ltd. (assignees of L. E. Norton). Convention date (U.S.A.) 26th February, 1945.

621 748.—A transmitter to be jettisoned by an aircraft and arranged to transmit position signals for directing rescue services.

The Decca Record Co. Ltd. (A communication from E. Fennessy). Application date 29th April, 1946.

622 711.—Electrical oscillations are fed to two full-wave rectifying meshes through an impedance, for modulation by another oscillation also fed to said meshes.

Philips Lamps Ltd. Convention date (Netherlands) 29th March, 1944.

623 430.—Self-excited oscillator in which modulation or control is effected by small changes in remote circuit elements giving an enhanced action by the Miller effect.

H. K. Neuber. Convention dates (U.S.A.) December 22nd, 1945 and December 11th, 1946.

623 741.—Frequency modulation for introducing auxiliary modulation or for increasing frequency deviation, wherein one modulated frequency is heterodyned with another modulated frequency, without demodulation being required.

Société Française Radio-Électrique. Convention date (France) March 17th, 1944.

624 341.—Reduction of amplitude modulation in f.m. systems wherein anode rectification in a valve is used to feed back a neutralizing amplitude-modulation component.

Western Electric Co. Inc. Convention date (U.S.A.) March 31st, 1939.

624 515.—Neutralizing of push-pull Lecher wire circuits is effected by feedback couplings provided by two series loops coupled to the input and output circuits.

Sadir-Carpentier. Convention date (France) April 26th, 1944.

624 936.—Carrier-shift keying using fixed-frequency and variable-frequency oscillators, a frequency-discriminator circuit operated by the two frequencies after mixing, controlling the variable oscillator.

The General Electric Co. Ltd. and J. B. L. Foot. Application date July 14th, 1947.

SIGNALLING SYSTEMS OF DISTINCTIVE TYPE

621 063.—Modulated pulse-communication system in which the leading and trailing edges of the pulses are time modulated by different signals.

Standard Telephones & Cables Ltd. (assignees of D. D. Grieg). Convention date (U.S.A.) 1st September, 1945.

621 850.—Motor operated a.f.c. system for telegraphic apparatus wherein marks and spaces are transmitted at different frequencies, the action of the motor being stopped in the event of weak signals.

Marconi's W.T. Co. Ltd. (assignees of H. O. Peterson). Convention date (U.S.A.) 2nd November, 1944.

623 415.—Multi-channel pulse communication system wherein pulses comprise several non-synchronized trains each having a characteristic width and recurrence frequency, the pulse-width being used at the receiver to separate the channels.

Standard Telephones & Cables Ltd. (assignees of E. Labin and D. D. Grieg). Convention date (U.S.A.) 26th February, 1945.

623 993.—Pulse-communication secrecy system in which audio signals frequency modulate a supersonic sub-carrier which, after conversion to f.m. pulses, modulate a transmitter.

The British Thomson-Houston Co. Ltd. (A Communication from the General Electric Co.). Application date 13th February, 1946.

624 514.—Multi-channel pulse communication receiver in which each channel selector selects the pulses of two or more non-adjacent channels, and includes a c.r.t. for distinguishing the two or more channels.

Standard Telephones and Cables Ltd. (assignees of E. Labin and D. D. Grieg). Convention date (U.S.A.) September 1st, 1945.

624 542.—Channel selector for pulse communication receiver in which a waveform of variable width is triggered by a sync pulse and is terminable only by the selected channel pulse.

Standard Telephones and Cables Ltd. (assignees of D. D. Grieg). Convention date (U.S.A.) March 2nd, 1946.

624 741.—Frequency-shift signalling system wherein a variable-frequency oscillator is controlled by a reactance tube itself controlled by signals, the coupling including a voltage-regulator device.

Marconi's W. Telegraph Co. Ltd. (assignees of H. E. Goldstine). Convention date (U.S.A.) January 29th, 1946.

CONSTRUCTION OF ELECTRON-DISCHARGE DEVICES

622 634.—Discharge device including a bunching resonator for partial velocity modulation of an electron stream, and a further bunching field coupled to a catching field.

Sperry Gyroscope Co. Inc. (assignees of R. H. Varian and W. W. Hansen). Convention date (U.S.A.) 22nd December, 1941.

622 826.—Klystron type valve wherein the electrodes are of segmental form separated by slots through which the electrons are directed in beams.

Société Française Radio Électrique. Convention date (France) 16th July, 1940.